



저작자표시-비영리-변경금지 2.0 대한민국

이용자는 아래의 조건을 따르는 경우에 한하여 자유롭게

- 이 저작물을 복제, 배포, 전송, 전시, 공연 및 방송할 수 있습니다.

다음과 같은 조건을 따라야 합니다:



저작자표시. 귀하는 원저작자를 표시하여야 합니다.



비영리. 귀하는 이 저작물을 영리 목적으로 이용할 수 없습니다.



변경금지. 귀하는 이 저작물을 개작, 변형 또는 가공할 수 없습니다.

- 귀하는, 이 저작물의 재이용이나 배포의 경우, 이 저작물에 적용된 이용허락조건을 명확하게 나타내어야 합니다.
- 저작권자로부터 별도의 허가를 받으면 이러한 조건들은 적용되지 않습니다.

저작권법에 따른 이용자의 권리는 위의 내용에 의하여 영향을 받지 않습니다.

이것은 [이용허락규약\(Legal Code\)](#)을 이해하기 쉽게 요약한 것입니다.

[Disclaimer](#)

Master's Thesis

Bismuth coated nanoporous carbon  
microelectrode-based heavy metal sensor

Soosung Kim

Department of Mechanical Engineering

Graduate School of UNIST

2018

Bismuth coated nanoporous carbon  
microelectrode-based heavy metal sensor

Soosung Kim

Department of Mechanical Engineering

Graduate School of UNIST

Bismuth coated nanoporous carbon  
microelectrode-based heavy metal sensor

A Thesis

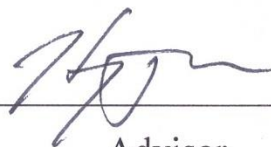
submitted to the Graduate School of UNIST

in partial fulfillment of the  
requirements for the degree of  
Master of Science

Soosung Kim

06/14/2018

Approved by



---

Advisor

Heungjoo Shin

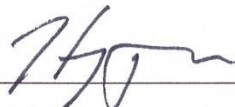
Bismuth coated nanoporous carbon  
microelectrode-based heavy metal sensor

Soosung Kim

This certifies that the thesis of Soosung Kim is approved.

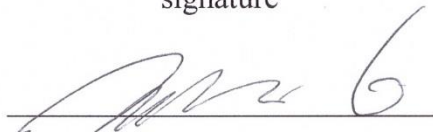
06/14/2018

signature



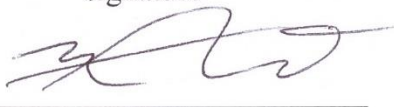
Advisor: Heungjoo Shin

signature



Jaesung Jang

signature



Hooneui Jeong

## Abstract

This study reports the development of an electrochemical heavy metal sensor based on nanoporous carbon electrodes (NPCEs) coated with Bi nanodendrites (BiNDs) for simultaneous heavy metal ion sensing. This sensor provides high sensitivity (3.151 for Cd(II) and 2.380 mA·L/μg·cm<sup>2</sup> for Pb(II) ions) along the linear range from 2 to 200μg/L of concentration for both ions and low limit of detection (0.827 and 1.121μg/L for Cd(II) and Pb(II) ions respectively). Such performance was achieved using BiND/NPCE structure, which offers enhanced electrochemical reaction and high surface area to volume ratio. This novel electrochemical heavy metal sensor was fabricated via simple batch processes based on carbon-MEMS, O<sub>2</sub> plasma etching and electroplating techniques. Original forms of the polymer precursors of NPCEs were fabricated by conventional UV lithography. After O<sub>2</sub> plasma etching process, then hierarchical porous structures were composed on the surface of the prepared polymer patterns. After pyrolysis, carbonization process of the polymer precursors under high temperature in vacuum, sponge-like NPCEs were build up. Insulation was also conducted via batch processes using UV lithography to expose the only sensor area (400μm-Ø) for quantitative measurement of heavy metal ions and wet etching method with buffered oxide etchant (BOE) with time controllability of etching rate for SiO<sub>2</sub> insulation layer. And simple electroplating was applied on the NPCEs in the solution containing bismuth ions. Bismuth is a promising functional material for electrochemical heavy metal sensors because of nontoxic material properties and comparable heavy metal sensing performance to mercury-based sensors which was developed and studied in the past. As for the measurement technique, square wave anodic stripping voltammetry (SWASV) method was utilized. In this method, Cd(II) and Pb(II) ions are reduced on the surface of BiND/NPCE and then

oxidized to generate peak currents at each redox potential. The complicated structure and material properties of BiNDs satisfied two main important factors of SWASV. Large surface area was composed in the shape of nanodendrites using Bi electroplating on the sponge-like surface of NPCEs. And material properties of bismuth accomplished high performance of SWASV without generating toxic wastes unlike Hg-based electrochemical heavy metal sensors. Thus, BiND/NPCE-based heavy metal sensor suggests a novel, simple, cost-effective and environment-friendly approach to the area of environmental monitoring technology.

### List of figures

**Figure 1.** (a) Square wave parameters, (b) potential application and (c) resulting current in square wave anodic stripping voltammetry.

**Figure 2.** Schematic of anodic stripping voltammetric heavy metal detection using ex-situ and in-situ Bi electroplating methods.

**Figure 3.** Schematics of the bulk fabrication and anodic stripping voltammetry of heavy metal sensors based on (a) 3D honeycomb-like N-doped carbon nanosheet framework decorated with bismuth nanoparticles [49] and (b) Bi nanosheet modified glassy carbon electrode [50].

**Figure 4.** SEM images of surface morphology of (a) reduce graphene oxide-carbon nanotube composite electrode [50] and (b) multi-walled carbon nanotube electrode [53].

**Figure 5.** SEM images of surface morphology of (a) Au nanoparticles coated chitosan-graphene/glassy carbon composite electrode [58] and (b) Ag nanoparticles coated screen-printed carbon electrode [63].

**Figure 6.** Schematic fabrication steps of nanoporous carbon using carbon-MEMS and O<sub>2</sub> plasma etching; (a) polymer patterning using UV-lithography, (b) nanopore formation on the polymer surfaces using O<sub>2</sub> plasma etching, and (c) pyrolysis [66].

**Figure 7.** SEM surface images of (a) SU-8 polymer structures treated by O<sub>2</sub> plasma etching for 300s and corresponding (b) pyrolyzed nanoporous carbon [66].

**Figure 8.** Schematic of experimental setup.

**Figure 9.** Schematic of the fabrication steps for NPCEs.

**Figure 10.** Potential application of 2-step ex situ Bi electroplating.

**Figure 11.** SEM images of the surface of porous carbon disk electrode by oxygen plasma etching time; 100 (a), 200 (b), 300 and (d) 400 s (d).



**Figure 12.** Cyclic voltammograms of the electrodes with 50mv/s in 0.2 M K<sub>2</sub>SO<sub>4</sub> solution by O<sub>2</sub> plasma etching time; bare, 100, 200 and 300 s treated.

**Figure 13.** SEM images of the surface of BiND/NPCE; (a) under -1.4 V for 60 s, followed by under -0.8V for (b) 60, (c) 120, (d) 180, (e) 240, (f) 300, (g) 360 and (h) 420 s for each in 0.1 M NaAc-HAc (pH 4.5) with 1 mM Bi(III).

**Figure 14.** SWASV plots of 100 µg/L Pb(II) sensing (a) and peak currents (b) by 2nd Bi electroplating time in 0.1 M NaAc-HAc (pH 4.5) with 1 mM Bi(III); Preconcentration time, 300 s; Preconcentration potential, -1.4 V; Scan range, -1.4 V → -0.5 V; Amplitude, 25 mV; Frequency, 15 Hz; step potential, 5 mV.

**Figure 15.** SWASV plots of 100 µg/L Cd(II) & Pb(II) sensing (a) and peak currents (b) by pH level in 0.1 M NaAc-HAc; Preconcentration time, 300 s; Preconcentration potential, -1.4 V; Scan range, -1.4 V → -0.5 V; Amplitude, 25 mV; Frequency, 15 Hz; Step potential, 5 mV.

**Figure 16.** SWASV plots of 100 µg/L Cd(II) & Pb(II) sensing (a) and peak currents (b) by preconcentration potential in 0.1 M NaAc-HAc (pH 4.5); Preconcentration time, 300 s; Scan range, -1.4 V → -0.5 V; Amplitude, 25 mV; Frequency, 15 Hz; Step potential, 5 mV.

**Figure 17.** SWASV plots of 100 µg/L Cd(II) & Pb(II) sensing (a) and peak currents (b) by preconcentration time in 0.1 M NaAc-HAc (pH 4.5); Preconcentration potential, -1.4 V; Scan range, -1.4 V → -0.5 V; Amplitude, 25 mV; Frequency, 15 Hz; Step potential, 5 mV.

**Figure 18.** SWASV plots (a), peak current density curves (b) and linear calibration curves (c) of Cd(II) and Pb(II) sensing by ion concentration in 0.1 M NaAc-HAc (pH 4.5); Preconcentration time, 300 s; Preconcentration potential, -1.4 V; Scan range, -1.4 V → -0.5 V; Amplitude, 25 mV; Frequency, 15 Hz; Step potential, 5 mV.

**Figure 19.** Performance of limit of detection (a) and sensitivity (b) of electrochemical heavy metal sensors.

### List of tables

**Table 1.** Limits, common sources and side effects of Cd(II) and Pb(II) ion concentration levels in drinking water and human blood.

**Table 2.** Summary of sensing performance of various Cd(II) and Pb(II) sensors.

**Contents**

<b>Abstract</b> .....	<b>5</b>
<b>List of figures</b> .....	<b>7</b>
<b>List of tables</b> .....	<b>9</b>
<b>Contents</b> .....	<b>10</b>
<b>I. Introduction</b>	
<b>1.1. Importance of heavy metal sensors</b> .....	<b>12</b>
<b>1.2. Conventional heavy metal detection methods</b> .....	<b>13</b>
<b>1.3. Electrochemical heavy metal sensors</b> .....	<b>15</b>
<b>1.4. Thesis outline</b> .....	<b>19</b>
<b>2. Experimental</b>	
<b>2.1. Reagents and apparatus</b> .....	<b>21</b>
<b>2.2. Preparation of NPCEs</b> .....	<b>22</b>
<b>2.3. BiND decoration</b> .....	<b>23</b>
<b>3. Results and discussion</b>	
<b>3.1 Morphology and characterization</b>	
<b>3.1.1. Morphology of NPCE</b> .....	<b>25</b>
<b>3.1.2. Effect of O<sub>2</sub> plasma etching on surface area</b> .....	<b>26</b>
<b>3.1.3. Morphology of BiNDs</b> .....	<b>28</b>
<b>3.1.4. Effect of Bi electroplating on heavy metal sensing</b> .....	<b>28</b>
<b>3.2. Optimization of sensing conditions</b>	
<b>3.2.1. pH level of target solution</b> .....	<b>29</b>
<b>3.2.2. Preconcentration potential</b> .....	<b>30</b>

<b>3.2.3. Preconcentration time</b>	<b>31</b>
<b>3.3. Heavy metal sensing performance</b>	
<b>3.3.1. Cd(II) and Pb(II) sensing performance</b>	<b>32</b>
<b>3.3.2. Evaluation</b>	<b>33</b>
<b>4. Conclusion</b>	<b>36</b>
<b>Reference</b>	<b>38</b>
<b>Acknowledgements</b>	<b>50</b>

## I. Introduction

### 1.1. Importance of heavy metal sensors

Heavy metals are the metal elements which has relatively higher atomic weight and specific gravity values than other metal elements with the general criteria of 63.5 and  $5\text{g/cm}^3$  for each. Small quantities of heavy metals are important for human health, since they are usually utilized to function as co-factors and prosthetic groups of many enzymes to maintain biochemical balance in human body [1]. However, excessive quantity of heavy metals resulting from unexpected continuous intake can be a great threat to human beings as well as environment [2]. Heavy metals are the most serious micropollutants and water pollutants that can cause serious environmental problems and severe organ damage because of their strong toxicity [3]. Among several kinds of heavy metal elements, cadmium (Cd) and lead (Pb) require special caution because they are easily exposed to environment in the form of industrial water wastes and air exhaust with highly toxic properties. The toxicity of Cd(II) and Pb(II) ions cause severe health problems such as human carcinogenesis, immune decline, gene mutation, genital disease and impaired neurobehavior, and they can be easily absorbed and accumulated in human bodies through various ways of environmental circulation such as air pollution, drinking water, soil, food, and use of industrial products [4, 5, 7 - 10]. In this reason, one of the representative international organizations, World Health Organization (WHO) has strongly suggested the data with the concrete guideline values of limiting concentration level in drinking water, as the only concentration level less than  $3\ \mu\text{g/L}$  for Cd(II) and  $10\ \mu\text{g/L}$  for Pb(II) ions should be included in drinking water to prevent their intrinsic danger resulting from toxicity [6].

<b>Metal</b>	<b>Limit in drinking water (µg/L)</b>	<b>Limit in human blood (µg/L)</b>	<b>Common sources</b>	<b>Side effects</b>	<b>Reference</b>
<b>Cd(II)</b>	<b>3</b>	<b>5</b>	<b>Batteries, pigments, paints, plastics, synthetic rubber, engraving and photographic process</b>	<b>Anaemia, hypertension, osteoporosis, lung cancer, osteomalacia, lymphocytosis, weight loss, kidney toxicity and pulmonary fibrosis</b>	<b>[7]</b>
<b>Pb(II)</b>	<b>10</b>	<b>50</b>	<b>Lead batteries, solders, agriculture, jewellery, PVC pipes and PVC lead paints</b>	<b>Kidney damage, Bone growth stagnation, rapid progress in Alzheimer's disease and senile dementia, IQ decline, ataxia and stupor</b>	<b>[8, 9, 10]</b>

Table 1. Limits, common sources and side effects of Cd(II) and Pb(II) ion concentration levels in drinking water and human blood.

In consideration of the severity of heavy metal pollution and its possible harms to humankind everywhere, therefore, active research and development of highly sensitive and accurate detection methods for Cd(II) and Pb(II) ions have been required for the environmental and food analysis. And there have been studied and invented a great many approaches to measure and analyze the heavy metal ions in the concentration level of µg/L and ng/L scale.

## 1.2. Conventional heavy metal detection methods

To analyze heavy metals in precision, a variety of scientific approaches had been developed and widely utilized. Methods for detection of heavy metals were continuously investigated through a lot of analytical technologies and instruments such as inductively coupled plasma-mass spectrometry

(ICP-MS) [11], inductively coupled plasma-atomic emission spectrometry (ICP-AES) [12], inductively coupled plasma-optical emission spectrometry (ICP-OES) [13], cold vapor atomic fluorescence spectrometry (CV-AFS) [14], atomic absorption spectrometry (AAS), atomic emission spectrometry (AES) [15], flameless atomic spectrometry (FAAS) [16], atomic fluorescence spectrometry (AFS) [17], and X-ray fluorescence (XRF) [18]. These techniques have shown highly sensitive performance and great selectivity for heavy metal detection so far. However, most of these methods require the expensive, bulky and complex machines and wide spaces enough to set them up. In addition, to run a set of analysis for heavy metal sensing, there should be a well-trained analyst for complicated operational procedures [19]. Moreover, it takes long time to implement the pretreatment process of heavy metal contained samples for measurement as well as detection step itself. Because of these inconvenience in time, space and money, on-site detection of heavy metals in environmental sample such as ground water cannot help being limited by, so to speak, the conventional heavy metal detection techniques introduced so far. To efficiently prevent the harms from heavy metal pollution and analyze the heavy metal contaminants in the way of on-site detection, there needs to be some essential characteristics such as portable set up of instrumentation, simple pretreatment of heavy metal pollutant samples, short time measurement and direct monitoring. To realize and satisfy these conditions, there needed to be invented a new way of approach to measure heavy metal elements with comparably highly sensitive detection performance and excellent selectivity. Therefore, a novel and simple heavy metal sensing technology was invented and it is called electrochemical heavy metal detection, which operates based on potentiometric input and corresponding current signals resulting from electrochemical reaction between a sensor and heavy metal ions. Since electrochemical heavy metal detection overcame the limits of conventional technologies, it has been established as a powerful alternative method.

### 1.3. Electrochemical heavy metal sensors

For the cost-effective and simple detection of heavy metals, electrochemical sensors have been actively studied with high sensitivity, selectivity, and simple configuration. Among various electrochemical detection methods, square wave anodic stripping voltammetry (SWASV) allows high sensitivity by accumulating target metal ions on the working electrodes in the preconcentration steps [20]. In addition, quantitative multi-target detection is conducted by measuring anodic currents during scanning stripping voltage, as shown in Figure 1. SWASV facilitates good detection limits because of efficient discrimination of signals between the charge and the faradaic current with shorter preconcentration times [21].

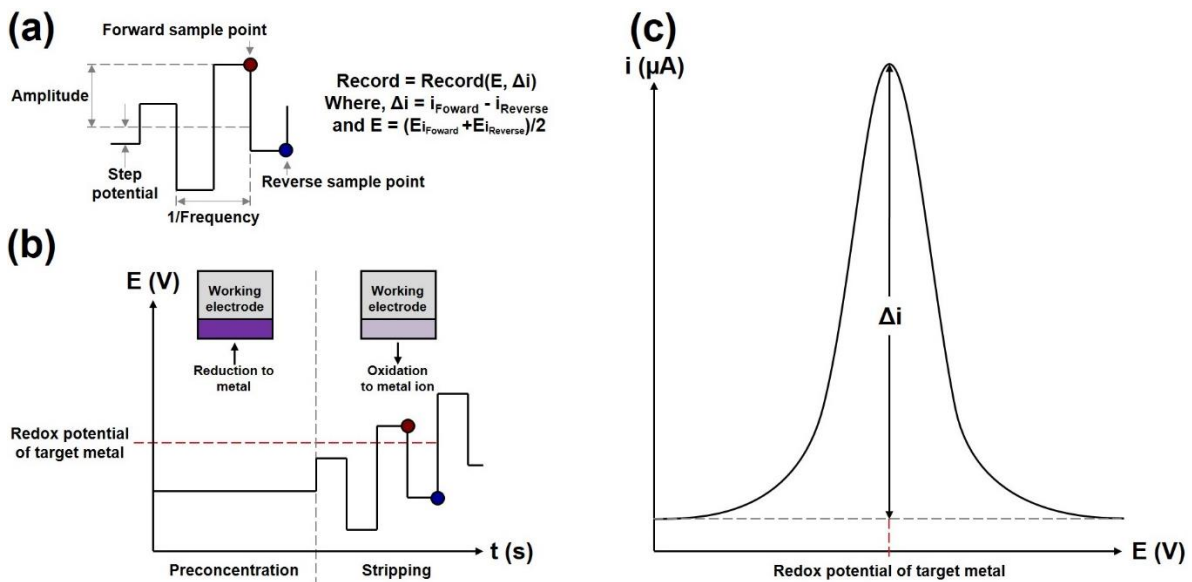


Figure 1. (a) Square wave parameters, (b) potential application and (c) resulting current in square wave anodic stripping voltammetry.

As the heavy metal sensor electrode material in stripping voltammetry, mercury has been



primarily utilized because of its good negative potential range for the reduction of various heavy metal ions, which prevents solvent electrolysis [22]. However, the toxicity of mercury requires special caution and limits its applications to reusable sensors and continuous monitoring of food and water [23]. Regarding these concerns, other alternative materials such as gold, silver or iridium has been utilized [24 - 26]. Even if these substitutionary electrodes don't cause toxic wastes, overall performance has not reached that of Hg electrodes with distorted stripping peak and large background current. Instead, bismuth turned out to be a proper alternative electrode material for mercury, since it has comparable stripping performances for heavy metal detection and exhibits low toxicity [27, 28]. Bismuth also exhibits advantages such as high sensitivity, great resolution of neighboring peaks, well-defined peaks, broad cathodic potential range, reproducible stripping performance, insensitivity to dissolved oxygen and wide linear range. [29 - 35]. This phenomenon comes from the preconcentrating step on Bi electrodes [36]. Like as amalgam formation of Hg electrodes, there occurs the formation of multi-component alloy with low melting temperature between bismuth and various heavy metals such as gallium, thallium, antimony, indium as well as cadmium or lead. Therefore, methods to compose bismuth on the substrate had to be taken into designing of Bi-based electrodes [37, 38]. To fabricate Bi-based electrodes, there are three general methods including Ex situ electroplating, in situ electroplating and bulk method. Ex situ and in situ electroplating methods both Bi electroplating techniques, but required steps and solution conditions are different as shown in Figure 2. Ex situ electroplating technique is pre-plating method before sensing experiment. The electrode to decorate is immersed into Bi(III) solution for application of the potential enough low to reduce Bi(III) onto the working electrode surface [39 - 42]. Ex situ electroplating method has advantages that Bi(III) mixing and controlling processes are not required for preconcentration step during sensing test. But there should be additional process of Bi electroplating in

fabrication. For in situ electroplating method, the solution utilized in sensing contains not only heavy metal ions but also Bi(III) ions in supporting electrolyte [43 - 45]. In situ electroplating method does not need the separate Bi electroplating process other than ex situ electroplating process. However there needs to be optimization for controlling the concentration of Bi(III) ion in presence with heavy metal ions, as well as additional mixing step of target solution of heavy metal ions.

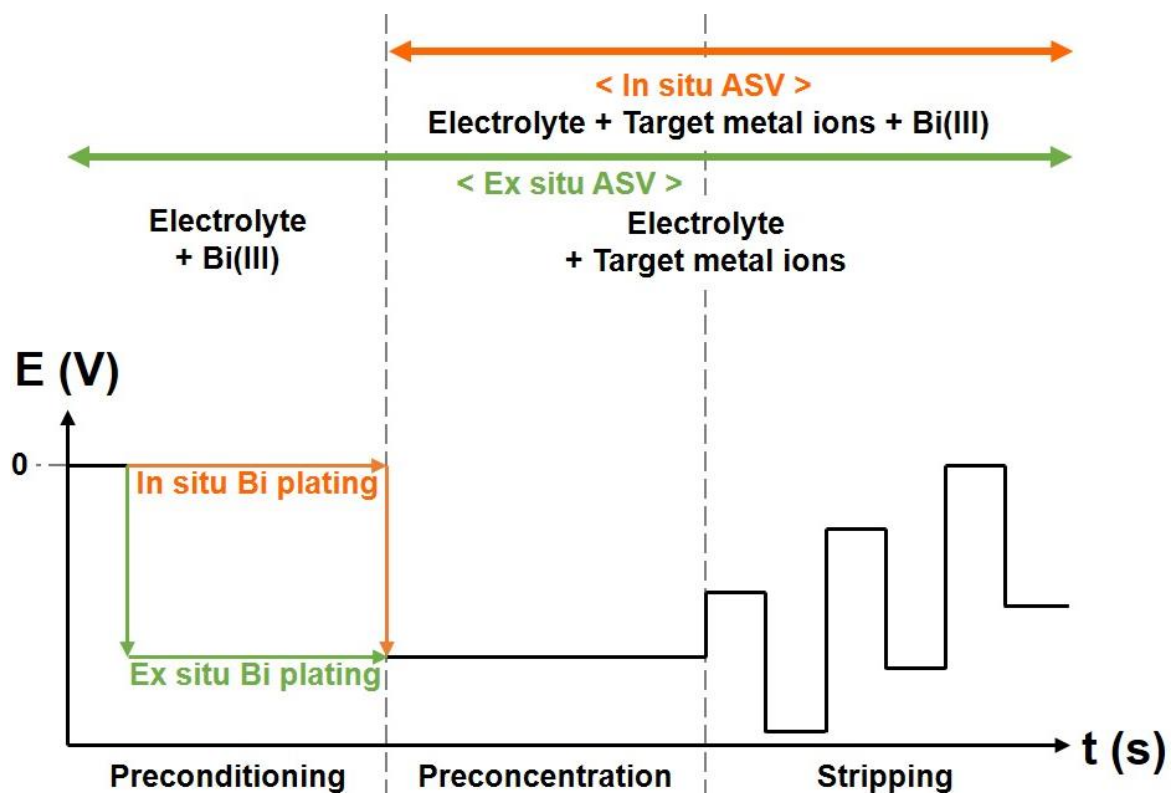


Figure 2. Schematic of anodic stripping voltammetric heavy metal detection using ex situ and in situ Bi electroplating methods.

The last way to fabricate Bi-based electrode is called bulk method. In-bulk method, modification of working electrodes with Bi is conducted during preparation of mixture or solution to produce Bi composite electrodes through synthesis or screen-printing technique [46 - 49]. Bi is physically added or applied by chemical reaction in bulk method as shown in Figure 3. So bulk

method has the advantage that there is no need for control of Bi electroplating solution and parameter optimization. But, synthesis-based bulk method takes long time and complicated chemical reaction processes.

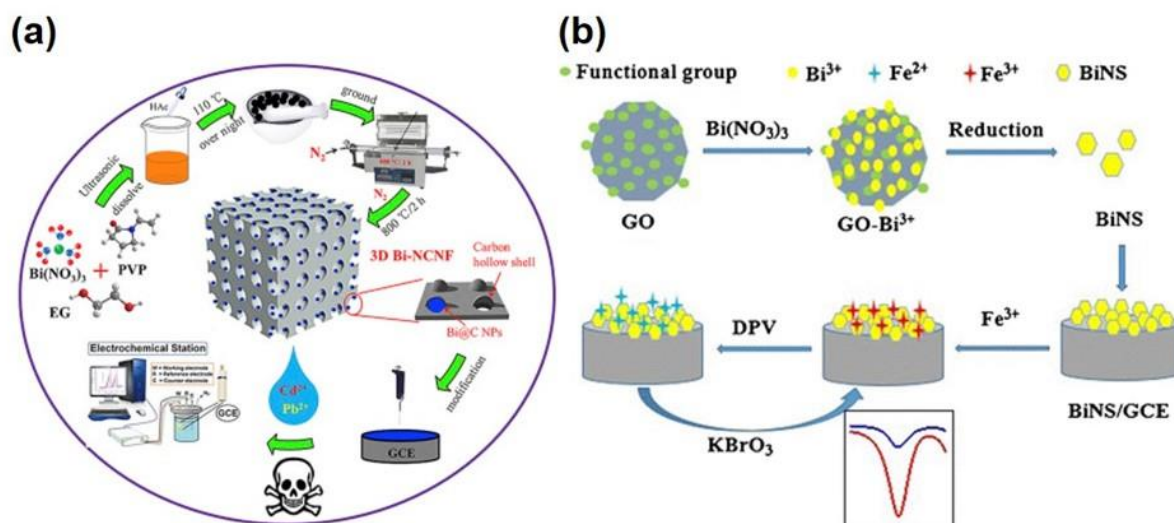


Figure 3. Schematics of the bulk fabrication and anodic stripping voltammetry of heavy metal sensors based on (a) 3D honeycomb-like N-doped carbon nanosheet framework decorated with bismuth nanoparticles [49] and (b) Bi nanosheet modified glassy carbon electrode [50].

To enhance the performance as well, fabrication processes for increased surface area of electrode have been developed such as porous composite electrodes synthesized using reduced graphene, carbon nanotube [51 - 57] or other nanoparticles [58 - 66] in suspension or solution phase as shown in Figure 4 and 5. However, these are hard to apply batch process. Also, screen printing method has limitation of porosity at the electrode surface and synthetic approach lead to inevitable complexity and longtime in processes. Because of these problems there needs to be a novel approach for electrochemical heavy metal sensors via batch fabrication method.

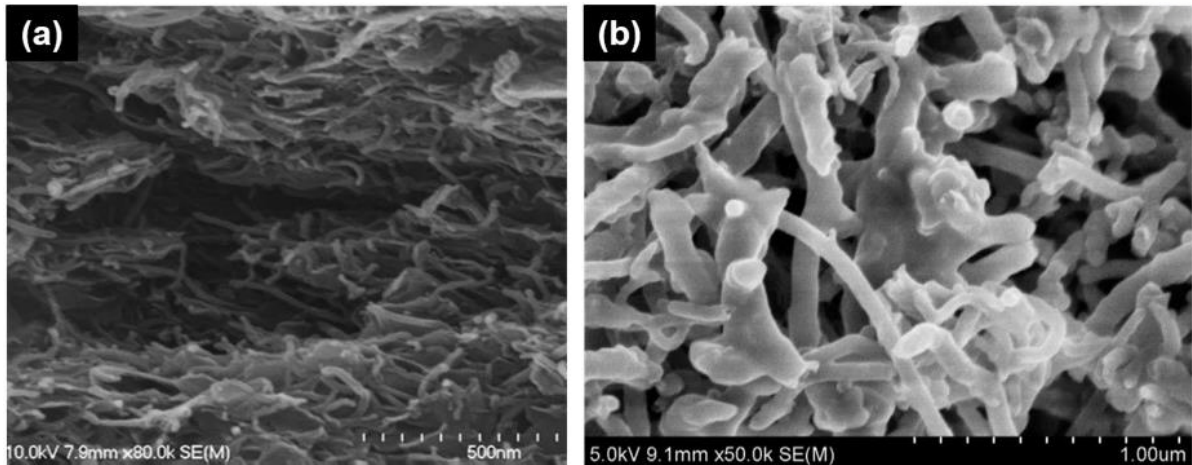


Figure 4. SEM images of surface morphology of (a) reduce graphene oxide-carbon nanotube composite electrode [51] and (b) multi-walled carbon nanotube electrode [54].

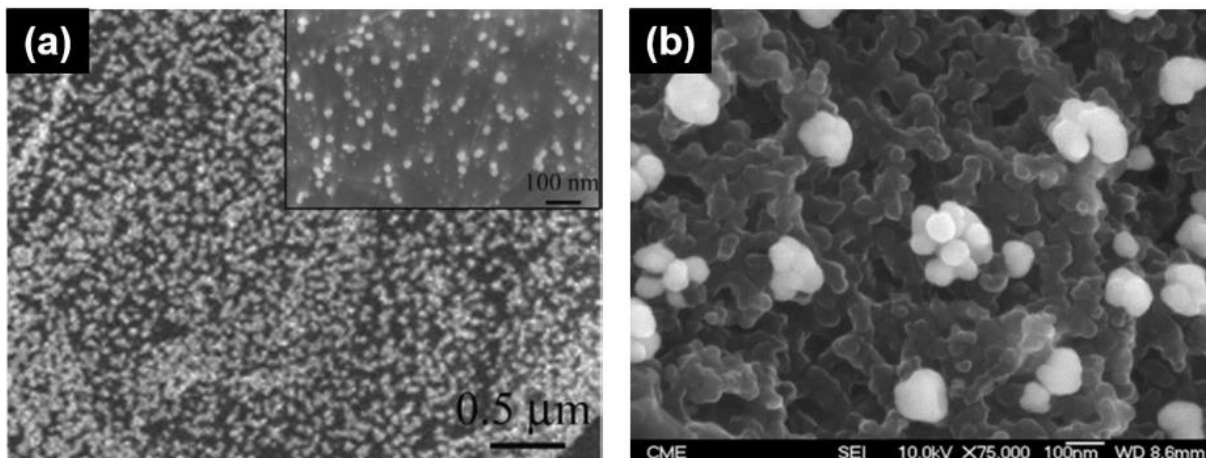


Figure 5. SEM images of surface morphology of (a) Au nanoparticles coated chitosan-graphene/glassy carbon composite electrode [59] and (b) Ag nanoparticles coated screen-printed carbon electrode [64].

#### 1.4. Thesis outline

In this work, a highly sensitive and reliable electrochemical heavy metal sensor based on BiND integrated NPCE was newly developed via batch fabrication method in a 6-inch wafer scale. The Bi-coated NPCE was fabricated using only batch fabrication methods. Polymer structures were patterned using photolithography and then hierarchical porous surface was formed via O<sub>2</sub> plasma etching process. Due to the isotropic etching and self-mask effect, nanoporous carbon surface was

formed in the shape of sponge-like network. Finally, the porous patterns were converted into NPCEs via pyrolysis [67]. After insulating the electrode except the sensing area, bismuth was selectively electroplated in the form of hierarchical nanodendrites on the NPCEs. The large surface area resulting from the hierarchical nanostructures performed highly sensitive detection of dual heavy metal ions using SWASV technique.

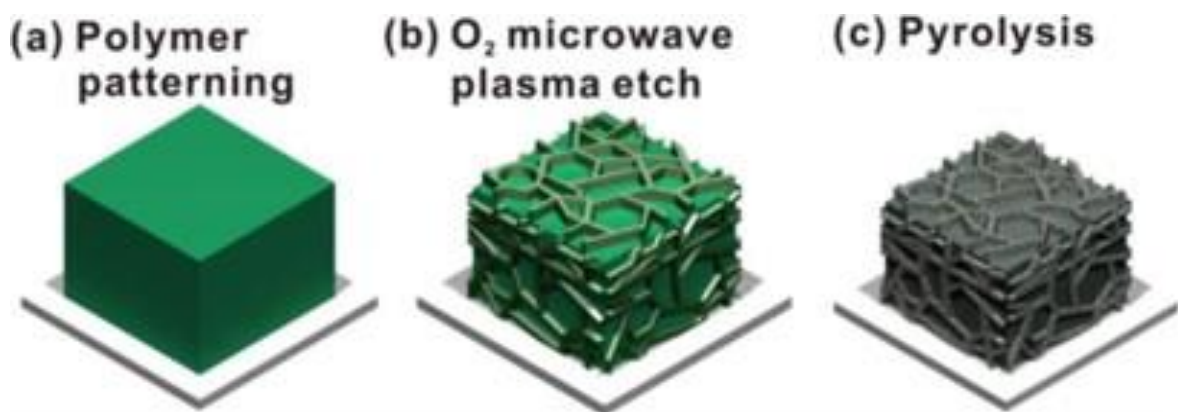


Figure 6. Schematic of fabrication of nanoporous carbon using carbon-MEMS and O<sub>2</sub> microwave plasma etching [67].

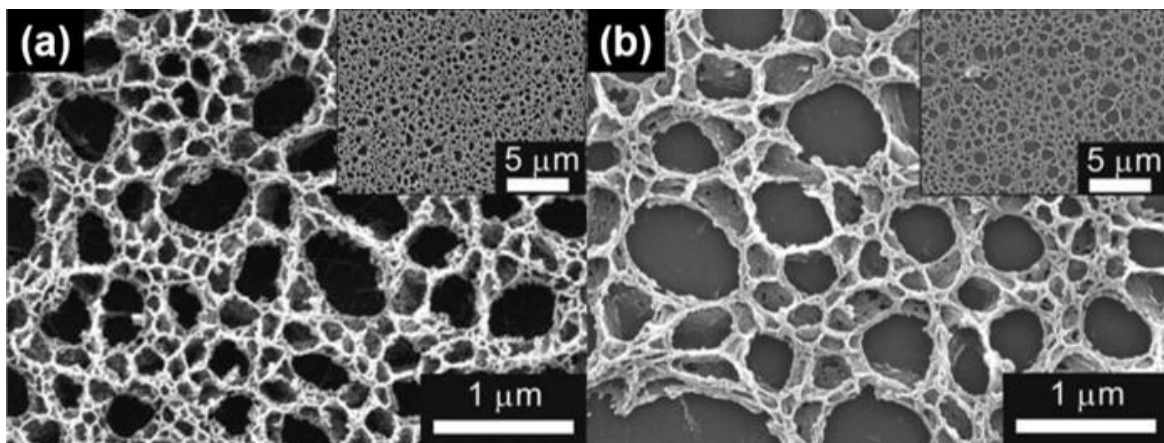


Figure 7. SEM surface images of (a) SU-8 polymer structures treated by O<sub>2</sub> plasma etching for 300s and corresponding (b) pyrolyzed nanoporous carbon [67].

## 2. Experimental

### 2.1. Reagents and apparatus

All reagents utilized throughout this study are analytical grade purity. For conventional UV lithography, two photoresists were prepared. SU-8 3035, a negative photoresist was purchased from MicroChem. AZ 9260, a positive photoresist was purchased from MicroChemicals. Potassium sulfate powder (99.0 %), cadmium (II) and lead (II) standard stock solutions (1000 mg/L) were purchased from Sigma-Aldrich. Bismuth (III) standard stock solution (1000 mg/L) was purchased from Kanto Chemicals. Acetic acid (99.7 %) and sodium acetate trihydrate (99.5 %) were purchased from Samchun Chemicals. As for the experimental instruments, UV lithography processes were conducted using a mask aligner (MA6, SUSS MicroTec AG, Germany). O<sub>2</sub> plasma etching was processed by a PR asher (V15-G, KAMI, Germany). Plasma enhanced chemical vapor deposition (PECVD) process for insulation layer integration was done using a PECVD machine (PEH-600, SORONA Inc., Republic of Korea). Surface morphology of electrode sample was investigated by a scanning electron microscope (Quanta 200, FEI Co., USA). All the electrochemical experiments were set up with three-electrode configuration with BiND/NPCE, platinum wire and Ag/AgCl as working, counter and reference electrodes for each. Electrochemical characterization was examined using a multi-potentiostat (CHI 1020; CH Instrument Inc., USA). Heavy metal ion detection was done using a potentiostat (IviumStat, Ivium Technologies, Netherlands). And heavy metal sensing performance was implemented as shown in Figure 8.

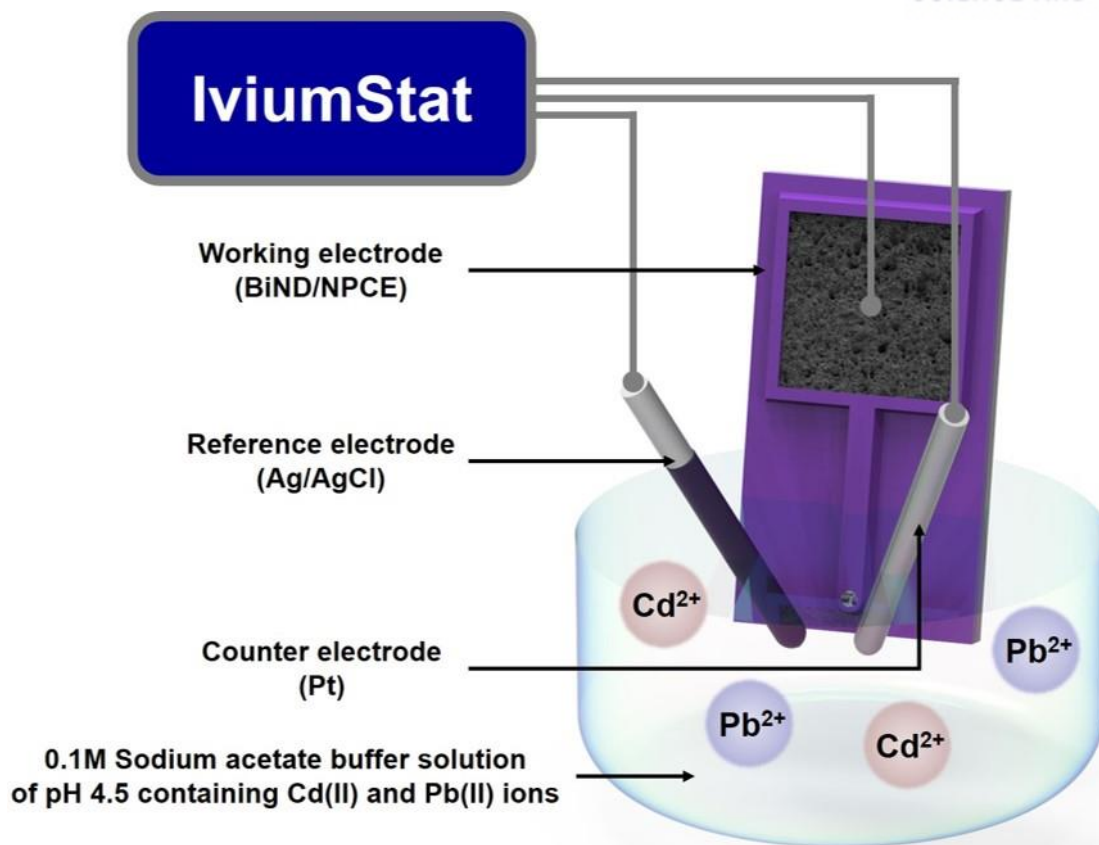


Figure 8. Schematic of experimental setup.

## 2.2. Preparation of NPCEs

NPCEs were fabricated via carbon-MEMS and O<sub>2</sub> plasma etching techniques. At first, 1- $\mu\text{m}$ -thick SiO<sub>2</sub> insulation layer deposited 6-inch Si wafer was prepared as a substrate by wet oxidation, followed by cleaning with hot piranha solution and dehydration at 200°C for 5 min on a hot plate. 30- $\mu\text{m}$ -thick SU-8 negative photoresist was spin coated on the substrate and soft-baked on a hot plate for 11 min at 95°C and cooled in room temperature. Then, micro-sized polymer structures were patterned by UV exposure using a mask aligner and baked at 95°C for 7 min on a hot plate. After developing process, the polymer structures got etched by O<sub>2</sub> plasma for 100, 200 and 300s with the power of 500 W with 60 sccm O<sub>2</sub> at 50Pa. In this process, metal ions such as antimony ions in the SU-8 polymer precursors functioned as etch-mask from O<sub>2</sub> plasma [67]. Then, there composed the hierarchical porous

surface structures on the polymer precursors. Carbonization of the precursors was done through pyrolysis process under vacuum at high temperature as much as 900°C in a furnace. The pyrolyzed glassy carbon electrodes were produced with sponge-like nanoporous carbon network on the surface. For insulation, 30nm-thick-SiO<sub>2</sub> layer was deposited by PECVD process. Square-shaped connection pad and active circle area got open by UV lithography of 10-μm-thick AZ positive photoresist and wet etching process based on BOE to finally fabricate the NPCEs with batch processes in a 6-inch wafer scale.

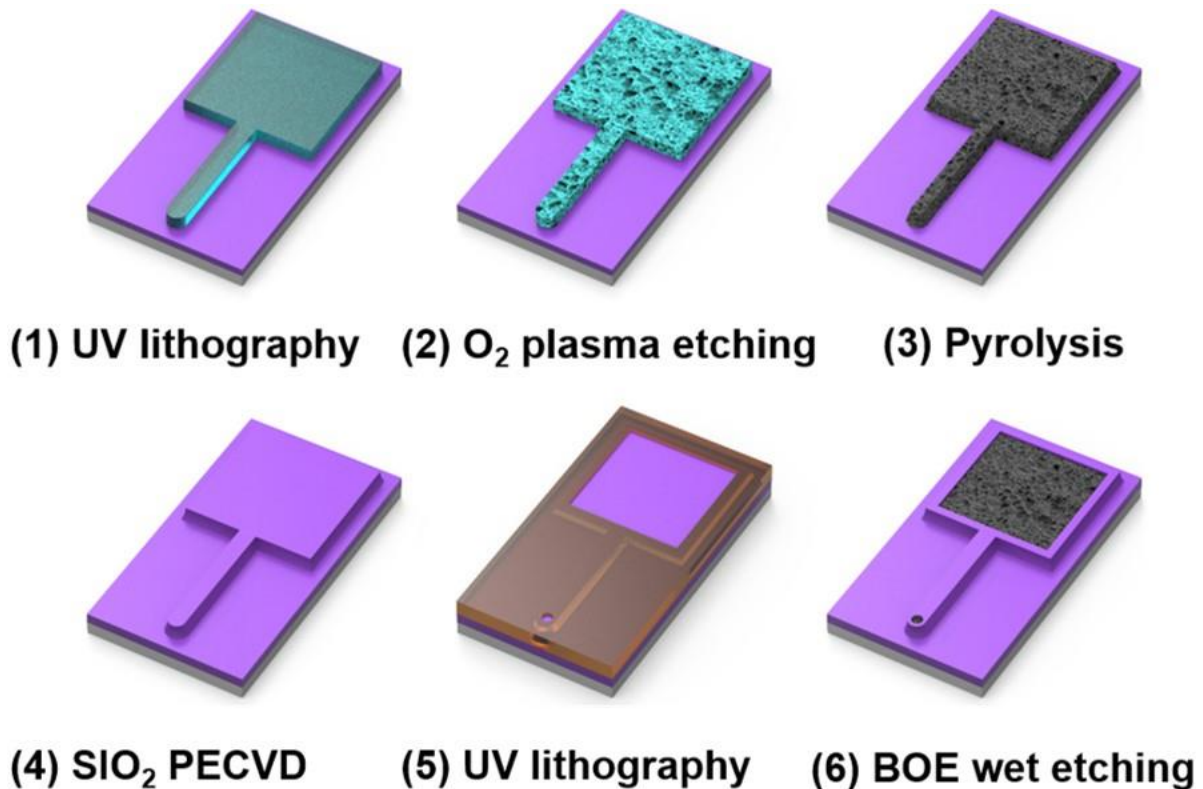


Figure 9. Schematic of the fabrication of NPCEs.

### 2.3. BiND decoration

BiNDs were decorated on the NPCEs by simple electroplating method. In 0.1 M sodium



acetate buffer solution (NaAc-HAc) of pH 4.5 with 1mM Bi(III), 2-step ex situ Bi electroplating process was applied on the NPCEs with platinum wire and Ag/AgCl electrode for counter electrode and reference electrode. To compose evenly grown Bi seeds on the carbon surface, the potential of -1.4 V was applied for 60 s in the first step. In the second step, -0.8 V was loaded for 60, 120, 180, 240, 300, 360 and 420 s for densely grown BiNDs with volume. After rinsing with deionized water and drying, fabrication of BiND/NPCEs was completed.

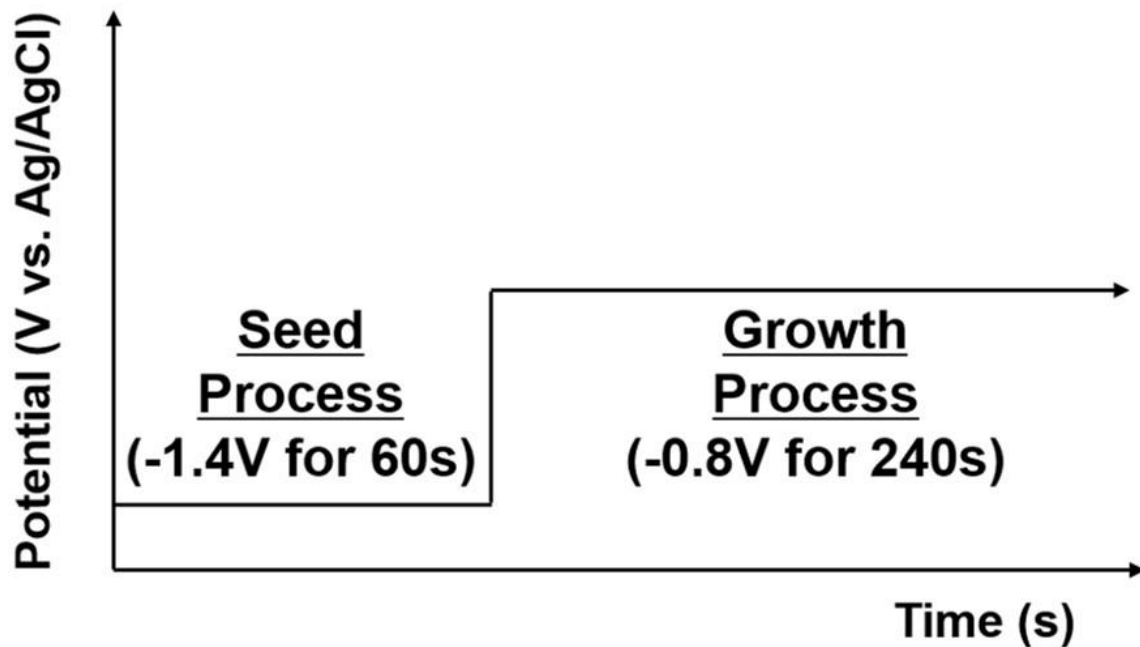


Figure 10. Potential application of 2-step ex situ Bi electroplating.

### 3. Results and discussion

#### 3.1 Morphology and characterization

##### 3.1.1. Morphology of NPCE

The surface morphology of NPCE was observed using scanning electron microscope. Due to O<sub>2</sub> plasma etching process, hierarchical porous carbon networks were successfully formed on the surface of pyrolyzed carbon electrodes. As shown in Figure 9, as more O<sub>2</sub> plasma etching time applied from 100 to 300 s, the number of pore increased and the size of pore decreased. The more processed under O<sub>2</sub> plasma etching, the deeper pores composed on the surface of the electrode. In other words, the number of smaller and deeper pores got augmented as the processing time increased. Among these SEM images, it seems to be the best porosity on the surface of the electrode etched for 300 s. Actually, the polymer precursors undergone O<sub>2</sub> plasma etching process for 400 s turned out to be over etched to be vanished accompanying loss of resultant electrode volume. This phenomenon shows etching time over 300 s is not desirable parameter with consideration of the function of the electrode. Unnecessary volume loss of the carbon resulting from excessive etching is supposed to be decline of electrochemical performance of the electrode. Thus, there can be told that the porosity of the surface of NPCE got higher as O<sub>2</sub> plasma etching process treated for longer time, but 300 s led to the best porosity without needless volume loss.

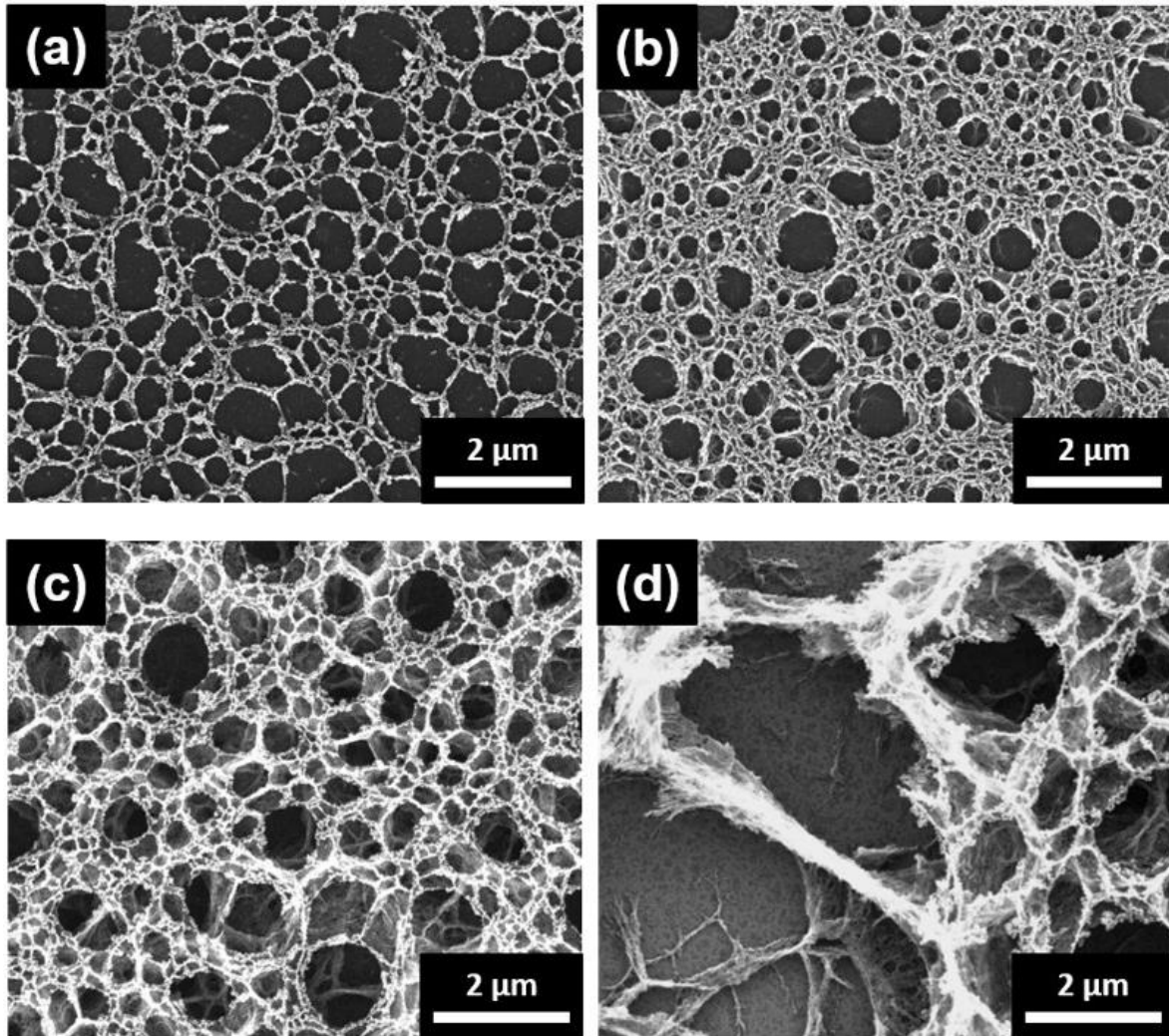


Figure 11. SEM images of the surface of porous carbon disk electrode by oxygen plasma etching time; 100 (a), 200 (b), 300 and (d) 400 s (d).

### 3.1.2. Effect of O<sub>2</sub> plasma etching on surface area

The effect on electrochemical behavior of the composed nanoporous surface of carbon electrodes by O<sub>2</sub> plasma etching time was tested by cyclic voltammetry in 0.2M K<sub>2</sub>SO<sub>4</sub> solution with 50mV/s. As can be observed in Figure 10, the area of each plot got higher as the time of O<sub>2</sub> plasma etching increased from 0 (Bare) to 300 s. And the electrochemical performance of NPCEs can be digitized in a form of specific areal capacity as the formula indicates, where E1 and E2 are switching potentials in cyclic voltammetry, A means the nominal open area of electrodes (Diameter = 400 μm)

and  $v$  is scan rate, 50 mV/s.

$$C = \frac{\int_{E_1}^{E_2} i(E) dE}{2(E_2 - E_1)Av}$$

As a result of calculation of each plot, the specific areal capacity values were 0.369 for bare carbon, 0.509 for 100 s treated, 1.610 for 200 s treated and 2.012 mF/cm<sup>2</sup> for 300 s treated carbons by O<sub>2</sub> plasma etching process. This phenomenon demonstrates the more time O<sub>2</sub> plasma etched nanoporous carbon got more enlarged surface area for electrochemical reaction. Therefore, the nanoporous carbon was set to be fabricated under O<sub>2</sub> plasma etching for 300 s as it showed the best electrochemical performance and surface area to volume ratio.

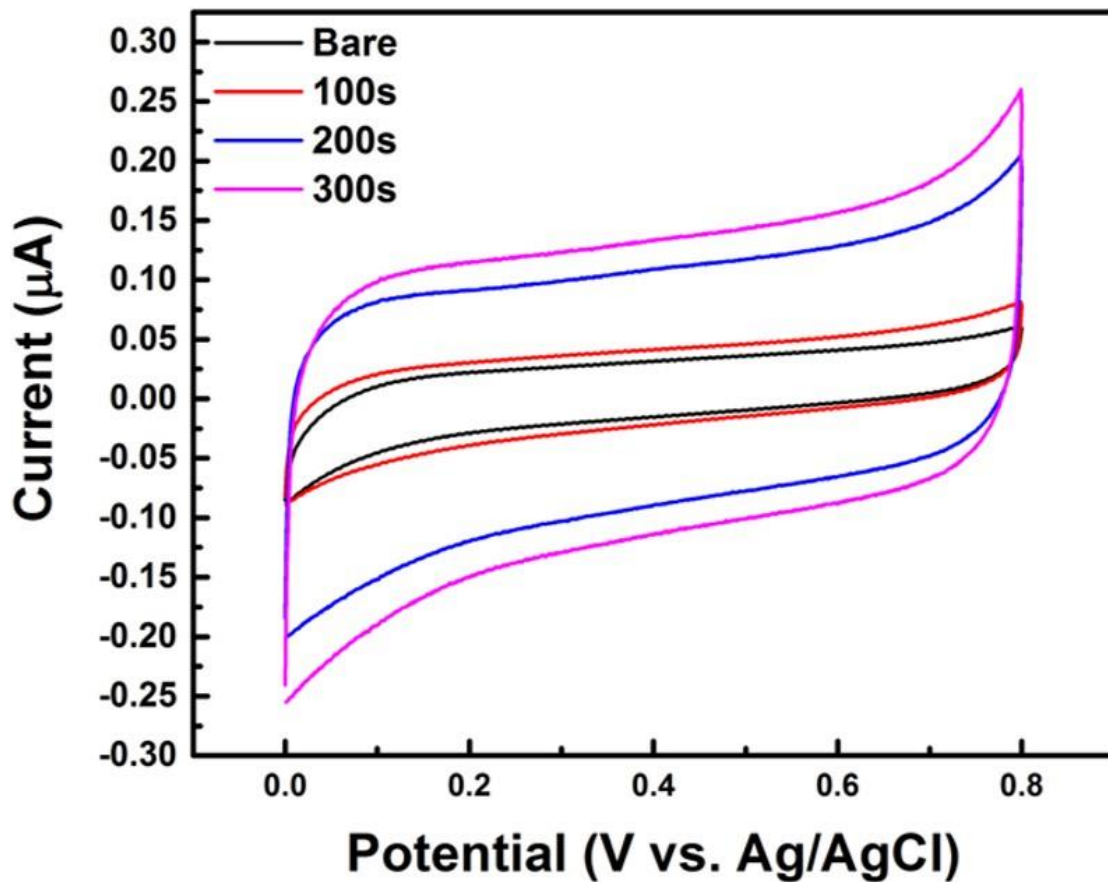


Figure 12. Cyclic voltammograms of the electrodes with 50mv/s in 0.2 M K<sub>2</sub>SO<sub>4</sub> solution by O<sub>2</sub> plasma etching time; bare, 100, 200 and 300 s treated.

### 3.1.3. Morphology of BiNDs

For investigation of BiNDs on the NPCEs by applied time of electroplating, different times under  $-0.8\text{ V}$  were applied on the NPCEs. At first, the morphology of Bi dendrites was checked with electron scanning microscope. As shown in Figure 11(a), for 1st step Bi electroplating under  $-1.4\text{ V}$  for  $60\text{ s}$ , Bi seeds were evenly grown on the walls of NPCE surface. And from Figures 11b to 11h, the volume and density of BiNDs seemed like getting higher as applied time increased, however, there could not be evaluated about significant difference from  $240\text{ s}$ . There seems to be saturation of BiNDs on the top surface, since the electrical charge got concentrated and Bi electroplating reaction got to be occurred on the top branches without Bi ions reaching the lower parts in BiND network.

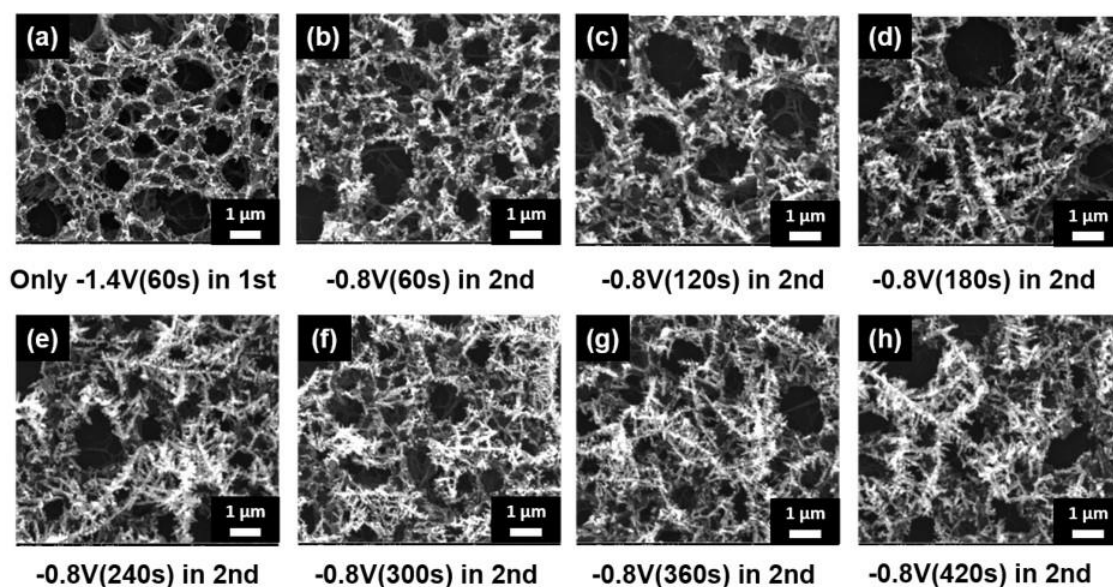


Figure 13. SEM images of the surface of BiND/NPCE; (a) under  $-1.4\text{ V}$  for  $60\text{ s}$ , followed by under  $-0.8\text{ V}$  for (b)  $60$ , (c)  $120$ , (d)  $180$ , (e)  $240$ , (f)  $300$ , (g)  $360$  and (h)  $420\text{ s}$  for each in  $0.1\text{ M NaAc-HAc}$  ( $\text{pH } 4.5$ ) with  $1\text{ mM Bi(III)}$ .

### 3.1.4. Effect of Bi electroplating on heavy metal sensing

The actual sensing performance by 2nd Bi electroplating time was examined using SWASV,

in 0.1 M NaAc-HAc of pH 4.5 with 100  $\mu\text{g/L}$  Pb(II). NaAc-HAc was selected as the supporting electrolyte, since this is commonly used buffer solution for anodic stripping voltammetry, with capacity to be applied to environmental samples [29]. Peak current value got increased by 2nd Bi electroplating time got longer as shown in Figure 12. By the way, the current value along time showed saturation tendency after 180 s. With the consideration of Bi morphology over the applied electroplating time, from 180 s, the BiNDs got saturated and there occurs the only top surface reaction without reaching inside bismuth dendrite network. Since the electric charge was getting concentrated on the top part, electroplating reaction ran on the only top surface of the BiNDs.

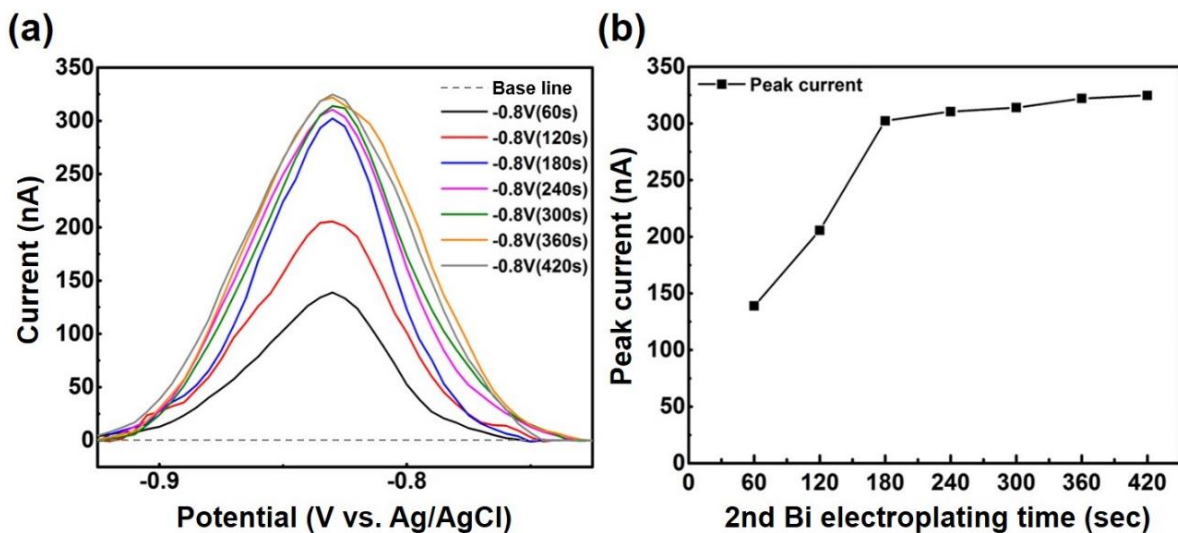


Figure 14. SWASV plots of 100  $\mu\text{g/L}$  Pb(II) sensing (a) and peak currents (b) by 2nd Bi electroplating time in 0.1 M NaAc-HAc (pH 4.5) with 1 mM Bi(III); Preconcentration time, 300 s; Preconcentration potential, -1.4 V; Scan range, -1.4 V  $\rightarrow$  -0.5 V; Amplitude, 25 mV; Frequency, 15 Hz; Step potential, 5 mV.

### 3.2. Optimization of sensing conditions

#### 3.2.1. pH level of target solution

To figure out the optimal pH level of supporting electrolyte, sodium acetate buffer, the sensing

performance by pH level was examined as shown in Figure 13. Both of Cd(II) and Pb(II) ions showed maximized peak current values where the pH level of solution was 4.5. The pH levels too lower or higher than pH 4.5 couldn't generate the maximized SWASV performance of BiND/NPCEs. This phenomenon could be attributed to the increased hydrogen evolution at the interface between BiND/NPCE and the solution can interfere with preconcentration of the target metal ions in lower acidity than optimal level [68]. In higher pH level than 4.5, peak currents decreased by lowering the acidity of the solution, since hydrolysis of Bi(III) increased [69]. Thus, pH 4.5 was set to be optimized value for heavy metal sensing measurement.

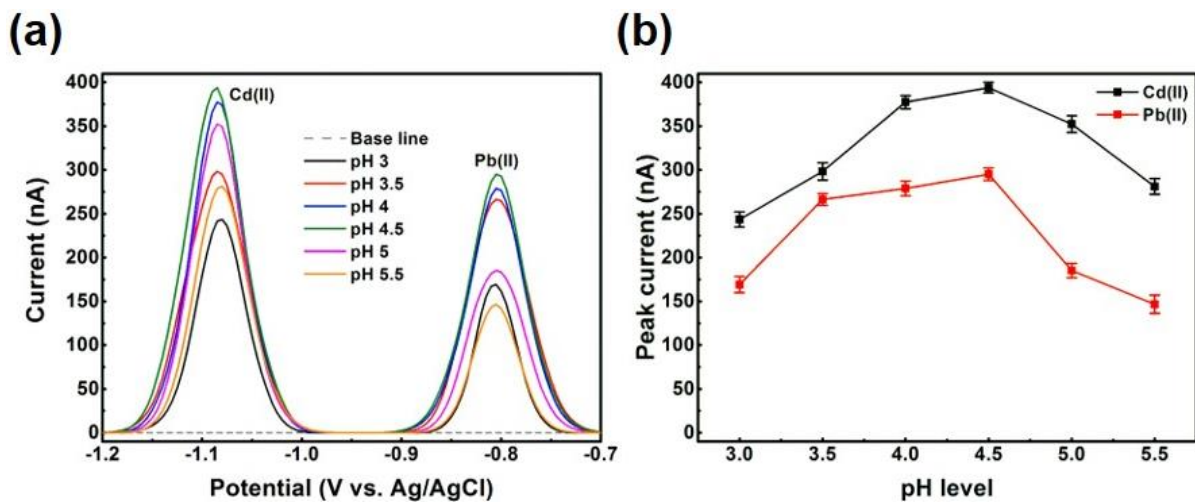


Figure 15. SWASV plots of 100  $\mu\text{g/L}$  Cd(II) & Pb(II) sensing (a) and peak currents (b) by pH level in 0.1 M NaAc-HAc; Preconcentration time, 300 s; Preconcentration potential, -1.4 V; Scan range, -1.4 V  $\rightarrow$  -0.5 V; Amplitude, 25 mV; Frequency, 15 Hz; Step potential, 5 mV.

### 3.2.2. Preconcentration potential

To get optimized sensing conditions, the experiment of varying preconcentration potential was conducted in 0.1 M NaAc-HAc of pH 4.5 as supporting electrolyte with 100  $\mu\text{g/L}$  Cd(II) and Pb(II). Both Cd(II) and Pb(II) ions got the best responses under -1.4 V, as shown in Figure 14. Saturation

phenomenon could be observed as the potential get lowered considering the trend from -1.0 to -1.4 V, however during the application of -1.5 V, the hydrogen evolution rose excessively. The hydrogen reduction and resulting bubble could interfere with great preconcentration of Cd(II) and Pb(II). Therefore, the optimized preconcentration potential was set to be -1.4 V. And there hardly turned up Cd(II) peak currents in the case of -1.0 and -1.1 V applications. This was because the redox potential of Cd(II) in this reaction system is around -1.1 V. Those two conditions were not sufficient reduce Cd(II) on BiND/NPCE to get great stripping performance.

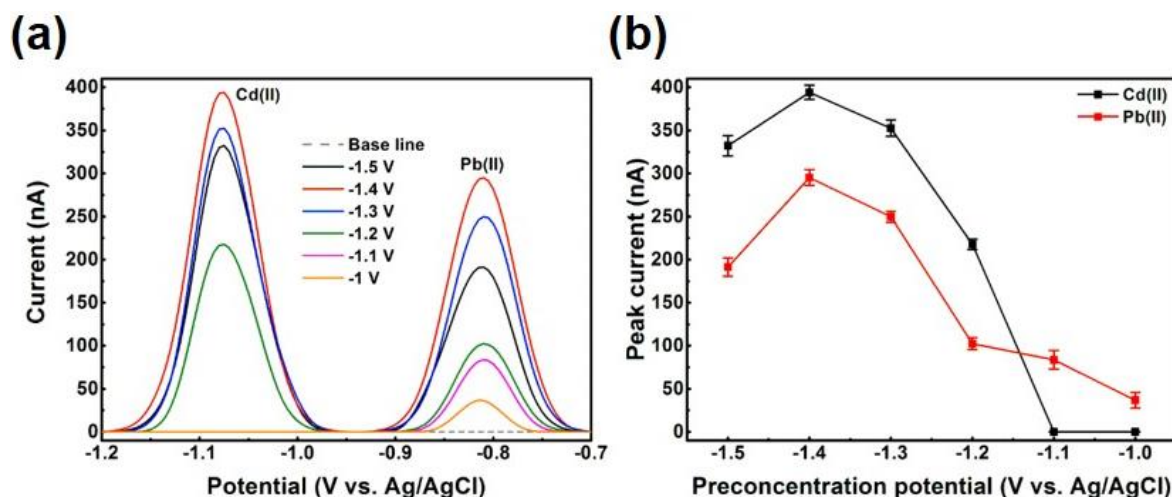


Figure 16. SWASV plots of 100 µg/L Cd(II) & Pb(II) sensing (a) and peak currents (b) by preconcentration potential in 0.1 M NaAc-HAc (pH 4.5); Preconcentration time, 300 s; Scan range, -1.4 V → -0.5 V; Amplitude, 25 mV; Frequency, 15 Hz; Step potential, 5 mV.

### 3.2.3. Preconcentration time

The time of preconcentration of target ions is also the controllable parameter in SWASV measurement. The peak current and applied preconcentrating time was tested for optimization process as well. As Figure 15 shows, the more preconcentration time goes, the larger peak current values were observed in SWASV results. By the way, the current values got saturated from 300 s approximately for



both Cd(II) and Pb(II) ions. The peak currents after 300 s did not get significant increase, instead the values were in similar level, compared with the values till 200 s for both Cd(II) and Pb(II) ions. This result is supposed that the nominal open area of the electrode ruled the saturation phenomenon during preconcentration process. Based on the result, the optimized value for preconcentration time was set to be 300 s.

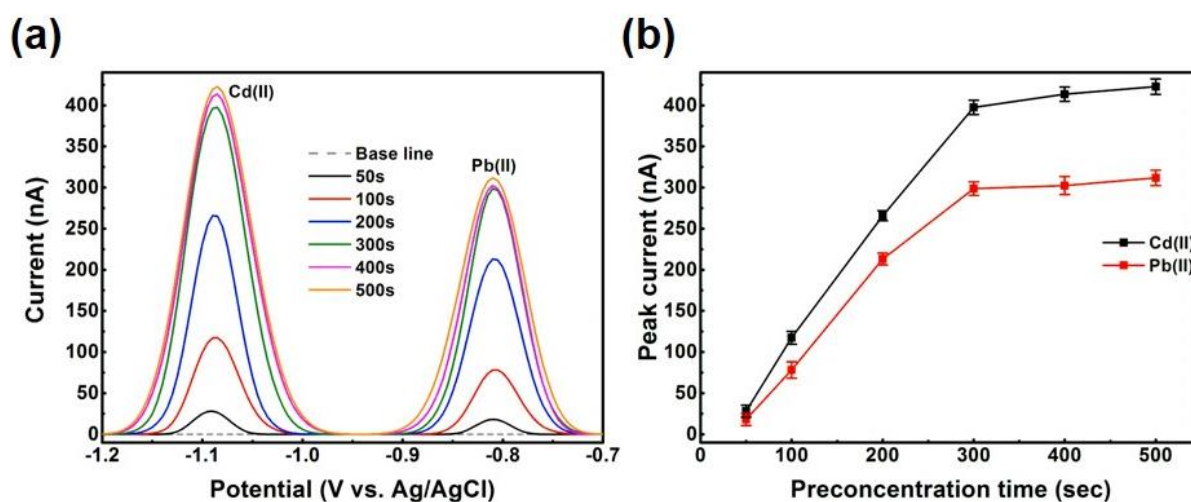


Figure 17. SWASV plots of 100  $\mu\text{g/L}$  Cd(II) & Pb(II) sensing (a) and peak currents (b) by preconcentration time in 0.1 M NaAc-HAc (pH 4.5); Preconcentration potential, -1.4 V; Scan range, -1.4 V  $\rightarrow$  -0.5 V; Amplitude, 25 mV; Frequency, 15 Hz; Step potential, 5 mV;

### 3.3. Heavy metal sensing performance

#### 3.3.1. Cd(II) and Pb(II) sensing performance

The performance of electrochemical heavy metal sensor based-on BiND/NPCE was examined by SWASV under the optimized conditions for simultaneous detection of Cd(II) and Pb(II) ions with different concentrations from 2 to 600  $\mu\text{g/L}$ . The saturation phenomenon occurred for both of the peak currents of Cd(II) and Pb(II) ions, as observed in Figure 16b. The target ions were saturated from 400  $\mu\text{g/L}$  for Cd(II) and from 200  $\mu\text{g/L}$  for Pb(II). This phenomenon is also assumed that the

nominal open area with 400 $\mu\text{m}$  of diameter limited the linearity over concentration levels of Cd(II) and Pb(II). The sensitivity values of the proposed sensor were 3.151 and 2.380  $\text{mA}\cdot\text{L}/\mu\text{g}\cdot\text{cm}^2$  in detection of Cd(II) and Pb(II) for each under the linear range between 2 to 200  $\mu\text{g}/\text{L}$ . The limit of detection values were calculated to be 0.827  $\mu\text{g}/\text{L}$  for Cd(II) and 1.121  $\mu\text{g}/\text{L}$  for Pb(II) (S/N=3).

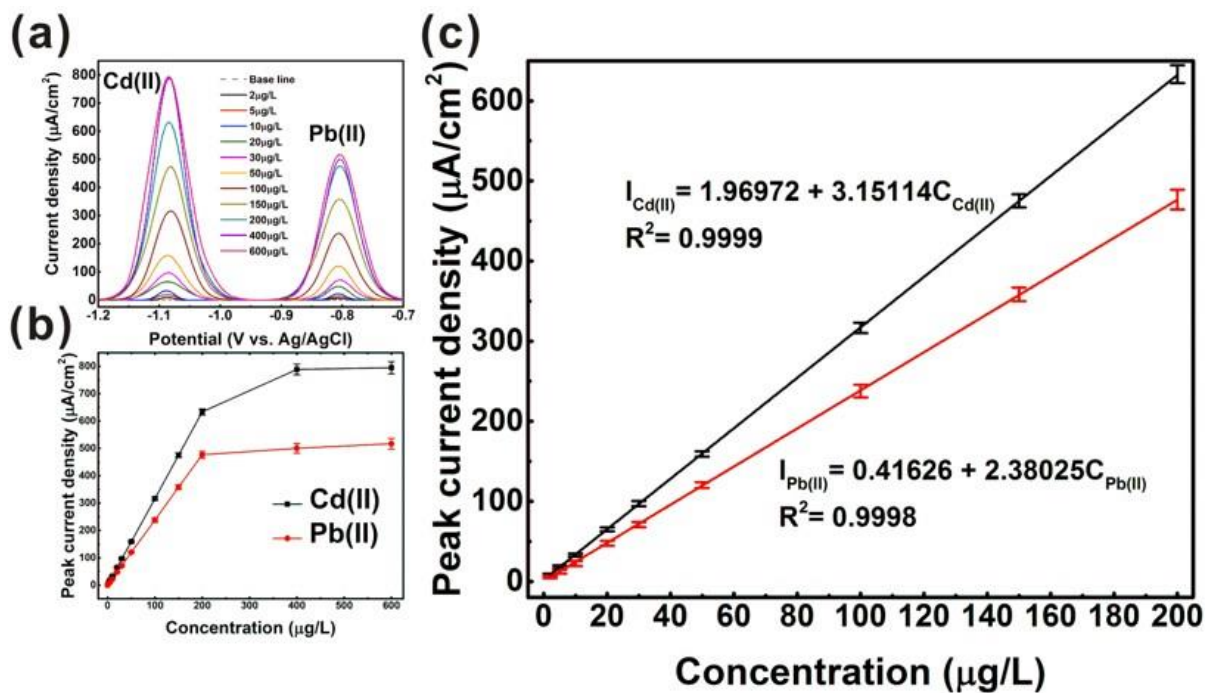


Figure 18. SWASV plots (a), peak current density curves (b) and linear calibration curves (c) of Cd(II) and Pb(II) sensing by ion concentration in 0.1 M NaAc-HAc (pH 4.5); Preconcentration time, 300 s; Preconcentration potential, -1.4 V; Scan range, -1.4 V  $\rightarrow$  -0.5 V; Amplitude, 25 mV; Frequency, 15 Hz; E step, 5 mV;

### 3.3.2. Evaluation

The proposed BiND/NPCE based-electrochemical heavy metal sensor got compared with other various electrochemical heavy metal sensors as shown in Figure 17 and Table 2. The proposed sensor showed low value of limit of detection and great sensitivity in comparable level among the other works. In regard to the simplicity of fabrication and capability of batch fabrication in wafer scale, this

work shows great efficiency over the other works. In other words, BIND/NPCE does not need to suffer the disadvantages as the other works need to endure the complexity and longtime paid for suspension or solution method of composite electrode processing or pretreatment of sample solution for in situ plating, the proposed electrochemical heavy metal sensor based-on BiND/NPCE shows competitive performance for its lower loads of fabrication processes.

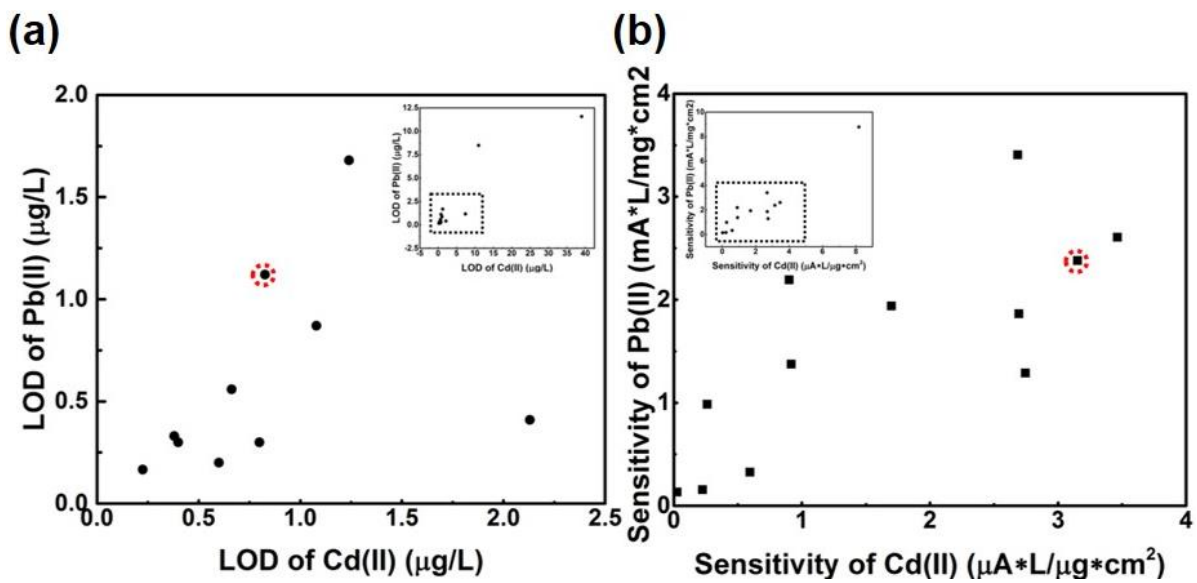


Figure 19. Performance of limit of detection (a) and sensitivity (b) of electrochemical heavy metal sensors.

Reference	Electrode	LOD		Sensitivity		Linear range	
		(μg/L)		(mA·L/μg·cm <sup>2</sup> )		(μg/L)	
		Cd(II)	Pb(II)	Cd(II)	Pb(II)	Cd(II)	Pb(II)
[51]	Au/rGOCNT10-1/Bi	0.6	0.2	0.262	0.986	20-150	20-150
[54]	Engineered MWCNTs	0.4	0.3	2.69	1.9	2-50	2-50
[55]	CNF-Nafion/GCE	0.38	0.33	1.70	1.94	2-100	2-100
[56]	NCQDs-GO	7.45	1.17	0.23	0.16	11.24-11241	20.72-10360
[57]	Bi/ERNGO/GCE	0.23	0.17	8.18	8.78	1.124-112.4	2.07-207.2
[70]	PA/PPy/GO	2.13	0.41	0.92	1.38	5-150	5-150
[71]	Bi/IPA-treated CC	1.08	0.87	3.46	2.6	5-110	5-110
[72]	Alk-Ti <sub>3</sub> C <sub>2</sub> /GCE	11.02	8.50	0.90	2.19	11.24-168.62	20.72-310.8
[73]	N-PCNFs/Nafion/GCE	0.8	0.3	0.60	0.33	2-100	0.5-10
[74]	MgFe-LDH/graphene	0.66	0.56	2.7	3.4	11.24-112.41	20.72-207.2
[75]	Clicked-CoPc/GCE	39.01	11.58	0.03	0.14	0-11241.1	0-20720
[76]	Nafion coated Bi	1.24	1.68	2.75	1.29	10-50	10-50
<b>This work</b>	<b>BiND/NPCE</b>	<b>0.827</b>	<b>1.121</b>	<b>3.151</b>	<b>2.380</b>	<b>2-200</b>	<b>2-200</b>

Table 2. Summary of sensing performance of various Cd(II) and Pb(II) sensors.

#### 4. Conclusion

I have developed a novel electrochemical heavy metal sensor based on the patternable NPCE decorated with BiNDs for Cd(II) and Pb(II) sensing with high sensitivity ( $3.151 \text{ mA}\cdot\text{L}/\mu\text{g}\cdot\text{cm}^2$  for Cd(II) and  $2.380 \text{ mA}\cdot\text{L}/\mu\text{g}\cdot\text{cm}^2$  for Pb(II) ions), low limit of detection values (0.827 for Cd(II) and  $1.121 \mu\text{g}/\text{L}$  for Pb(II) ions). This BiND/NPCE was fabricated via batch microfabrication methods including carbon-MEMS,  $\text{O}_2$  plasma etching and simple electroplating methods. The electrochemical redox reaction performance was maximized owing to the enlarged surface area to volume ratio of BiNDs composed on the sponge-like nanoporous carbon network. This hierarchical bismuth structures led to the great electrochemical performance during preconcentration and stripping steps of Cd(II) and Pb(II) ions in SWASV process. The sensitivity and limit of detection for Cd(II) and Pb(II) ions of the proposed sensor demonstrated high performance by optimizing the conditions of Bi electroplating condition, pH level of sampled solution with the target ions, preconcentration potential and time. Thus, between 2 and  $200 \mu\text{g}/\text{L}$  concentration range, the BiND/NPCE-based heavy metal sensor showed comparable values of sensitivity and limit of detection to other various sensors. Furthermore, consideration of the simplicity and capacity of mass production during fabrication processes lit up the strength of the BiND modified NPCE sensor as well. The BiND/NPCE-based electrochemical heavy metal sensor exhibits excellent feasibility as a powerful Cd(II) and Pb(II) sensing and monitoring tool for simultaneous detection of multiple heavy metal ions. This novel approach can be expected to be improved by simply increasing nominal area of the working electrodes to prevent saturation phenomenon observed in several sets of experiments. Moreover, it can be a great contribution to the area of environmental monitoring technology to develop this sensor for one chip integration of three electrodes on the substrate by simply adding counter and reference electrodes to the introduced fabrication processes. This research will be a

promising approach to development of electrochemical heavy metal sensor based on the demonstrated strength of high sensitivity, and the advantages cost-effective and timesaving fabrication processes.

## Reference

- [1] D. Bagchi, M. Bagchi, S. J. Stohs, D. K. Das, S. D. Ray, C. A. Kuszynski, S. S. Joshi, H. G. Pruess, "Free radicals and grape seed proanthocyanidin extract: importance in human health and disease prevention", *Toxicology*, **148**, 187 - 197 (2000).
- [2] L. Järup, "Hazards of heavy metal contamination", *Br. Med. Bull.*, **68**, 167 - 182 (2003)
- [3] B. Bansod, T. Kumar, R. Thakur, S. Rana, I. Singh, "A review on various electrochemical techniques for heavy metal ions detection with different sensing platforms", *Biosens. Bioelectron.*, **94**, 443 - 455 (2017).
- [4] M. P. Waalkes, "Review - Cadmium carcinogenesis", *Mut. Res.*, **533**, 107 - 120 (2003).
- [5] M. F. M. Noh & I. E. Tothill, "Development and characterisation of disposable gold electrodes, and their use for lead(II) analysis", *Anal. Binoanal. Chem.*, **386**, 2095 - 2106 (2006).
- [6] WHO, "12. Chemical fact sheets", *Guidelines for Drinking Water Quality*, **4th edn**, World Health Organization, Geneva, Switzerland, (2011).
- [7] N. Ercal, G.O. Hande, A.B. Nukhet, "Toxic metals and oxidative stress. Part I: Mechanisms involved in metal induced oxidative damage", *Curr. Top. Med. Chem.*, **1**, 529 - 539 (2001).
- [8] L. Patrick, "Lead toxicity. Part II: The role of free radical damage and the use of antioxidants in the pathology and treatment of lead toxicity", *Altern. Med. Rev.*, **11**, 114 - 127 (2006).

- [9] A. S. Ettinger, A. G. Wengrovitz, “CHAPTER 2. ADVERSE HEALTH EFFECTS OF LEAD EXPOSURE IN PREGNANCY”, *Guidelines for the identification and management of lead exposure in pregnant and lactating women*, US Department of Health and Human Services, Atlanta (2010).
- [10] C. Liu, R. Bai, Q. San Ly, “Selective removal of copper and lead ions by diethylenetriamine-functionalized adsorbent: behaviours and mechanisms”, *Water Res.*, **42**, 1511 - 1522 (2008).
- [11] P. Corbisier, D. V. D. Lelie, B. Borremans, A. Provoost, V. D. Lorenzo, N. L. Brown, J. R. Lloyd, J. L. Hobman, E. Csoregi, G. Johansson, B. Mattiasson, "Whole cell- and protein-based biosensors for the detection of bioavailable heavy metals in environmental samples", *Anal. Chim. Acta.*, **387**, 235 - 244 (1999).
- [12] K. S. Rao, T. Balaji, T. P. Rao, Y. Babu, G. R. K. Naidu, “Determination of iron, cobalt, nickel, manganese, zinc, copper, cadmium and lead in human hair by inductively coupled plasma-atomic emission spectrometry”, *Spectrochim. Acta Part B*, **57**, 1333 - 1338 (2002).
- [13] A. M. Massadeh, A. A. Alomary, S. Mir, F. A. Momani, H. I. Haddad, Y. A. Hadad, “Analysis of Zn, Cd, As, Cu, Pb, and Fe in snails as bioindicators and soil samples near traffic road by ICP-OES”, *Environ. Sci. Pollut. Res. Int.*, **13**, 13424 - 13431 (2016).
- [14] P. R. Aranda, P. H. Pacheco, R. A. Olsina, L. D. Martineza, R. A. Gil, “Total and inorganic mercury determination in biodiesel by emulsion sample introduction and FI-CV-AFS after multivariate optimization”, *J. Anal. At. Spectrom.*, **24**, 1441 - 1445 (2009).



- [15] I. Narin, M. Soylak, L. Elci, M. Dogan, "Determination of trace metal ions by AAS in natural water samples after preconcentration of pyrocatechol violet complexes on an activated carbon column", *Talanta*, **52**, 1041 - 1046 (2000).
- [16] T. Daşbaşı, Ş. Saçmacı, N. Çankaya, C. Soykan, "A new synthesis, characterization and application chelating resin for determination of some trace metals in honey samples by FAAS", *Food Chem.*, **203**, 283 - 291 (2016).
- [17] D. Sanchez-Rodas, W. T. Corns, B. Chen, P. B. Stockwell, "Atomic Fluorescence Spectrometry: a suitable detection technique in speciation studies for arsenic, selenium, antimony and mercury", *J. Anal. At. Spectrom.*, **25**, 933 - 946 (2010).
- [18] W. T. Elam, J. W. Adams, K. R. Hudson, B. McDonald, J. V. Gilfrich, "Subsurface Measurement of Soil Heavy-Metal Concentrations with the SCAPS X-Ray Fluorescence (XRF) Metals Sensor", *Field Anal. Chem. Technol.*, **2**, 97 - 102 (1998).
- [19] M. B. Gumpu, S. Sethuraman, U. M. Krishnan, J. B. B. Rayappan, "A review on detection of heavy metal ions in water – An electrochemical approach", *Sens. Actuators B*, **213**, 515 - 533, (2015).
- [20] R. O. Kadara, I. E. Tohill, "Stripping chronopotentiometric measurements of lead(II) and cadmium(II) in soils extracts and wastewaters using a bismuth film screen-printed electrode assembly", *Anal. Bioanal. Chem.*, **378**, 770 - 775 (2004).
- [21] V. Kumar, W. R. Heineman, "Thin-Layer Square Wave Voltammetry and Square Wave Stripping Voltammetry", *Anal. Chem.*, **59**, 842 - 846 (1987).

- [22] X. Zhu, C. Gao, J. Choi, P. L. Bishop, C. H. Ahn, "On-chip generated mercury microelectrode for heavy metal ion detection", *Lab Chip*, **5**, 212 - 217 (2005).
- [23] D. Cargnelutti, L. A. Tabaldi, R. M. Spanevello, G. D. O. Jucoski, V. Battisti, M. Redin, C. E. B. Linares, V. L. Dressler, E. M. D. M. Flores, F. T. Nicoloso, V. M. Morsch, M. R. C. Schetinger, "Mercury toxicity induces oxidative stress in growing cucumber seedlings", *Chemosphere*, **65**, 999 - 1006 (2006).
- [24] J. Wang, B. Tian, "Mercury-Free Disposable Lead Sensors Based on Potentiometric Stripping Analysis at Gold-Coated Screen-Printed Electrodes", *Anal. Chem.*, **65**, 1529 - 1532 (1993).
- [25] Y. Bonfil, E. K. irowa-Eisner, "Determination of nanomolar concentrations of lead and cadmium by anodic-stripping voltammetry at the silver electrode", *Anal. Chim. Acta*, **457**, 285 - 296 (2002).
- [26] M. A. Nolan, S. P. Kounaves, "Microfabricated Array of Iridium Microdisks as a Substrate for Direct Determination of Cu<sup>2+</sup> or Hg<sup>2+</sup> Using Square-Wave Anodic Stripping Voltammetry", *Anal. Chem.*, **71**, 3567 - 3573 (1999).
- [27] X. Pei, W. Kang, W. Yue, A. Bange, W. R. Heineman, I. Papautsky, "Improving Reproducibility of Lab-on-a-Chip Sensor with Bismuth Working Electrode for Determining Zn in Serum by Anodic Stripping Voltammetry", *J. Electrochem. Soc.*, **161**, B3160 - B3166 (2014).
- [28] H. Xu, L. Zeng, D. Huang, Y. Xian, L. Jin, "A Nafion-coated bismuth film electrode for the determination of heavy metals in vegetable using differential pulse anodic stripping voltammetry: An alternative to mercury-based electrodes", *Food Chem.*, **109**, 834 - 839 (2008).

- [29] Z. Zou, A. Jang, E. Macknight, P. Wu, J. Do, P. L. Bishop, C. H. Ahn, "Environmentally friendly disposable sensors with microfabricated on-chip planar bismuth electrode for in-situ heavy metal ions measurement", *Sens. Actuators B*, **134**, 18 - 24 (2008).
- [30] G. Lee, H. Lee, C. Rhee, "Bismuth nano-powder electrode for trace analysis of heavy metals using anodic stripping voltammetry", *Electrochem. Commun.*, **9**, 2514 - 2518 (2007).
- [31] V. Rehacek, I. Hotovy, M. Vojs, "Bismuth-coated diamond-like carbon microelectrodes for heavy metals determination", *Sens. Actuators B*, **127**, 193 - 197 (2007).
- [32] V. Sosa, N. Serrano, C. Arino, J. M. Diaz-Cruz, M. Esteban, "Sputtered bismuth screen-printed electrode: A promising alternative to other bismuth modifications in the voltammetry determination of Cd(II) and Pb(II) ions in groundwater", *Talanta*, **119**, 348 - 352 (2014).
- [33] R. O. Kadara, I. E. Tohill, "Resolving the copper interference effect on the stripping chronopotentiometric response of lead(II) obtained at bismuth film screen-printed electrode", *Talanta*, **66**, 1089 - 1093 (2005).
- [34] K. Keawkim, S. Chuanuwatanakul, O. Chailapakul, S. Motomizu, "Determination of lead and cadmium in rice samples by sequential injection/ anodic stripping voltammetry using a bismuth film/crown ether/Nafion modified screen-printed carbon electrode", *Food Control*, **31**, 14 - 21 (2013).
- [35] N. Lezi, A. Economou, P. A. Dimovasilis, P. N. Trikalitis, "Disposable screen-printed sensors modified with bismuth precursor compounds for the rapid voltammetric screening of trace Pb(II) and Cd(II)", *Anal. Chim. Acta*, **728**, 1 - 8 (2012).

- [36] a) J. Krueger, P. Winkler, E. Luderitz, M. Luek, "Bismuth Alloys and Bismuth Compounds", *Ullmann's Encyclopedia of Industrial Technology*, **Vol. 3** (Ed: M. Grayson), Wiley, New York, (1978); b) G. G. Long, L. D. Freedman, G. O. Doak, "Bismuth and Bismuth Alloys", *Encyclopedia of Chemical Technology*, **Vol. 3** (Ed: M. Grayson), Wiley, New York (1978).
- [37] A. Economou, "Bismuth-film electrodes: recent developments and potentialities for electroanalysis", *Trends Anal. Chem.*, **24**, 334 - 340 (2005).
- [38] N. Serrano, A. Alberich, J. M. Díaz-Cruz, C. Ariño, M. Esteban, "Coating methods, modifiers and applications of bismuth screen-printed electrodes", *Trends Anal. Chem.*, **46**, 15 -29 (2013).
- [39] N. Serrano, J. M. Diaz-Cruz, C. Arino, M. Esteban, "Ex situ Deposited Bismuth Film on Screen-Printed Carbon Electrode: A Disposable Device for Stripping Voltammetry of Heavy Metal Ions", *Electroanal.*, **22**, 1460 - 1467 (2010).
- [40] E. A. Hutton, S. B. Hocevar, B. Ogorevc, " Ex situ preparation of bismuth film microelectrode for use in electrochemical stripping microanalysis", *Anal. Chim. Acta*, **537**, 285 - 292 (2005).
- [41] T. Zidaric, V. Jovanovski, E. Menarta, M. Zorko, M. Kolar, M. Veber, S.B. Hocevar, " Multi-pulse galvanostatic preparation of nanostructured bismuth film electrode for trace metal detection", *Sens. Actuators B*, **245**, 720 - 725 (2017).
- [42] C. L. Jost, L. M. Martos, L. Ferraz, P. C. Nascimento, "Sequential Voltammetric Determination of Uranium, Cadmium and Lead by Using the ex situ Bismuth Film Electrode: Application to Phosphate Fertilizers", *Electroanal.*, **28**, 287 - 295 (2016).

- [43] D. Demetriades, A. Economo, A. Voulgaropoulos, “A study of pencil-lead bismuth-film electrodes for the determination of trace metals by anodic stripping voltammetry”, *Anal. Chim. Acta*, **519**, 167 - 172 (2004).
- [44] A. Krolicka, R. Pauliukaite, I. Svancara, R. Metelka, A. Bobrowski, E. Norkus, K. Kalcher, K. Vytras, “Bismuth-film-plated carbon paste electrodes”, *Electrochem. Commun.*, **4**, 193 - 196 (2002).
- [45] M. Frena, I. Campestrini, O.C. de Braga, A. Spinelli, “In situ bismuth-film electrode for square wave anodic stripping voltammetric determination of tin in biodiesel”, *Electrochim. Acta*, **56**, 4678 - 4684 (2012).
- [46] R. Pauliukaite, S. B. Hoëvar, B. Ogorevc, J. Wang, “Characterization and Applications of a Bismuth Bulk Electrode”, *Electroanal.*, **16**, 719 - 723 (2004).
- [47] C. Kokkinos, A. Economou, I. Raptis, T. Speliotis, “Disposable mercury-free cell-on-a-chip devices with integrated microfabricated electrodes for the determination of trace nickel(II) by adsorptive stripping voltammetry”, *Anal. Chim. Acta*, **622**, 111 - 118 (2008).
- [48] C. Kokkinos, A. Economou, M. Koupparis, “Determination of trace cobalt(II) by adsorptive stripping voltammetry on disposable microfabricated electrochemical cells with integrated planar metal-film electrodes”, *Talanta*, **77**, 1137 - 1142 (2009).
- [49] Z. Lu, W. Dai, X. Lin, B. Liu, J. Zhang, J. Ye, J. Ye, “Facile one-step fabrication of a novel 3D honeycomb-like bismuth nanoparticles decorated N-doped carbon nanosheet frameworks: Ultrasensitive electrochemical sensing of heavy metal ions”, *Electrochimica. Acta*, **266**, 94 - 102 (2018).

- [50] X. Hu, D. Pan, M. Lin, H. Han, F. Li, "Graphene oxide-assisted synthesis of bismuth nanosheets for catalytic stripping voltammetric determination of iron in coastal waters", *Microchim. Acta*, **183**, 855 - 861 (2016).
- [51] X. Xuan, J. Y. Park, "A miniaturized and flexible cadmium and lead ion detection sensor based on micro-patterned reduced graphene oxide/carbonnanotube/bismuth composite electrodes", *Sens. Actuators B*, **255**, 1220 - 1227 (2018).
- [52] H. Wang, G. Zhao, Z. Zhang, Y. Yi, Zhiqiang Wang, G. Liu, "A Portable Electrochemical workstation using Disposable Screen-Printed Carbon Electrode decorated with Multiwall Carbon Nanotube-Ionic Liquid and Bismuth Film for Cd(II) and Pb(II) Determination", *Int. J. Electrochem. Sci.*, **12**, 4702 - 4713 (2017).
- [53] X. Xuan, M. D. F. Hossain, J. Y. Park, "Solvothermal-Assisted, Reduced-Graphene-Oxide-Modified Bismuth Electrode for an Electrochemical Heavy-Metal-Ion Sensor", *J. Nanosci. Nanotechnol.*, **16**, 1 - 4 (2016).
- [54] X. Li, H. Zhou, C. Fu, F. Wang, Y. Ding, Y. Kuang, "A novel design of engineered multi-walled carbon nanotubes material and its improved performance in simultaneous detection of Cd(II) and Pb(II) by square wave anodic stripping voltammetry", *Sens. Actuators B*, **236**, 144 - 152 (2016).
- [55] D. Qin, S. Gao, L. Wang, H. Shen, N. Yalikun, P. Sukhrov, T. Wangberg, Y. Zhao, X. Manat, G. Hu, "Three-dimensional carbon nanofiber derived from bacterial cellulose for use in a Nafion matrix on a glassy carbon electrode for simultaneous voltammetric determination of trace levels of Cd(II) and Pb(II)", *Microchim. Acta*, **184**, 2759 - 2766 (2017).

- [56] L. Li, D. Liu, A. Shi, T. You, "Simultaneous stripping determination of cadmium and lead ions based on the N-doped carbon quantum dots-graphene oxide hybrid", *Sens. Actuators B*, **255**, 1762 - 1770 (2018).
- [57] W. Ren, Y. Zhang, M. Li, "Sensitive Determination of Zn<sup>2+</sup>, Cd<sup>2+</sup> and Pb<sup>2+</sup> at Electrochemically Reduced Nanoporous Graphene Oxide/ Bismuth Film Electrode", *Int. J. Electrochem. Sci.*, **13**, 1331 - 1342 (2018).
- [58] E. Bernalte, C. M. Sanchez, E. P. Gil, "Gold nanoparticles-modified screen-printed carbon electrodes for anodic stripping voltammetric determination of mercury in ambient water samples", *Sens. Actuators B*, **161**, 669 - 674 (2012).
- [59] J. Gong, T. Zhou, D. Song, L. Zhang, "Monodispersed Au nanoparticles decorated graphene as an enhanced sensing platform for ultrasensitive stripping voltammetric detection of mercury(II)", *Sens. Actuators B*, **150**, 491 - 497 (2010).
- [60] S. L. Ting, S. J. Ee, A. Ananthanarayanan, K. C. Leong, P. Chen, "Graphene quantum dots functionalized gold nanoparticles for sensitive electrochemical detection of heavy metal ions", *Electrochim. Acta*, **172**, 7 - 11 (2015).
- [61] M. A. G. Rico, M. Olivares-Marin, E. P. Gil, "Modification of carbon screen-printed electrodes by adsorption of chemically synthesized Bi nanoparticles for the voltammetric stripping detection of Zn(II), Cd(II) and Pb(II)", *Talanta*, **80**, 631 - 635 (2009).
- [62] K. E. Toghill, G. G. Wildgoose, A. Moshar, C. Mulcahy, R. G. Compton, "The Fabrication and Characterization of a Bismuth Nanoparticle Modified Boron Doped Diamond Electrode and Its

- Application to the Simultaneous Determination of Cadmium(II) And Lead(II)", *Electroanal.*, **20**, 1731 - 1737 (2008).
- [63] S. E. W. Jones, F. W. Campbell, R. Baron, L. Xiao, R. G. Compton, "Particle Size and Surface Coverage Effects in the Stripping Voltammetry of Silver Nanoparticles: Theory and Experiment", *J. Phys. Chem. C*, **112**, 17820 - 17827 (2008).
- [64] O. D. Renedo, M. J. A. Martinez, "A novel method for the anodic stripping voltammetry determination of Sb(III) using silver nanoparticle-modified screen-printed electrodes", *Electrochem. Commun.*, **9**, 820 - 826 (2007).
- [65] A. M. Ashrafi, S. Cerovac, S. Mudric, V. Guzsvany, L. Husakova, I. Urbanova, K. Vytras, "Antimony nanoparticle-multiwalled carbon nanotubes composite immobilized at carbon paste electrode for determination of trace heavy metals", *Sens. Actuators B*, **191**, 320 - 325 (2014).
- [66] K. E. Toghill, L. Xiao, G. G. Wildgoose, R. G. Compton, "Electroanalytical Determination of Cadmium(II) and Lead(II) Using an Antimony Nanoparticle Modified Boron-Doped Diamond Electrode", *Electroanal.*, **21**, 1113 - 1118 (2009).
- [67] Y. Lim, J. Woo, S. G. Joo, H. Shin, "Patternable Nanoporous Carbon Electrodes for Use as Supercapacitors", *J. Electrochem. Soc.*, **163**, A1886 - A1892 (2016).
- [68] Z. Wang, G. Liu, L. Zhang, H. Wang, "Electrochemical detection of trace cadmium in soil using a Nafion/stannum film-modified molecular wire carbon paste electrodes", *Ionics*, **19**, 1687 - 93 (2013).



- [69] S. Lee, S. Bong, J. Ha, M. Kwak, S. Park, Y. Piao, "Electrochemical deposition of bismuth on activated graphene-nafion composite for anodic stripping voltammetric determination of trace heavy metals", *Sens. Actuators B*, **215**, 62 - 69 (2015).
- [70] H. Dai, N. Wang, D. Wang, H. Ma, M. Lin, "An electrochemical sensor based on phytic acid functionalized polypyrrole/graphene oxide nanocomposites for simultaneous determination of Cd(II) and Pb(II)", *Chem. Eng. J.*, **299**, 150 - 155 (2016).
- [71] A. A. Saeed, B. Singh, M. N. Abbas, E. Dempsey, "Evaluation of Bismuth Modified Carbon Thread Electrode for Simultaneous and Highly Sensitive Cd (II) and Pb (II) Determination", *Electroanal.*, **28**, 2205 - 2213 (2016).
- [72] X. Zhu, B. Liu, H. Hou, Z. Huang, K. M. Zeinu, L. Huang, X. Yuan, D. Guo, J. Hu, J. Yang, "Alkaline intercalation of Ti<sub>3</sub>C<sub>2</sub>MXene for simultaneous electrochemical detection of Cd(II), Pb(II), Cu(II) and Hg(II)", *Electrochim. Acta*, **248**, 46 - 57 (2017).
- [73] S. Gao, C. Xu, N. Yalikun, X. Mamat, Y. Li, T. WAgberg, X. Hu, J. Liu, J. Luo, G. Hu, "Sensitive and Selective Differential Pulse Voltammetry Detection of Cd(II) and Pb(II) Using Nitrogen-Doped Porous Carbon Nanofiber Film Electrode", *J. Electrochem. Soc.*, **164**, H967 - H974 (2017).
- [74] Y. Ma, Y. Wang, D. Xie, Y. Gu, X. Zhu, H. Zhang, G. Wang, Y. Zhang, H. Zhao, "Hierarchical MgFe-layered double hydroxide microsphere/graphene composite for simultaneous electrochemical determination of trace Pb(II) and Cd(II)", *Chem. Eng. J.*, **347**, 953 - 962 (2018).

- [75] G. Fomo, N. Nwaji, T. Nyokong, “Low symmetric metallophthalocyanine modified electrode via click chemistry for simultaneous detection of heavy metals”, *J. Electroanal. Chem.*, **813**, 58 - 66 (2018).
- [76] L. Wang, G. Jing, T. Cui, “Nafion coated flexible bismuth sensor for trace lead and cadmium determination”, *Microsyst. Technol.*, **24**, 1 - 8 (2018).

## Acknowledgements

I extend my cordial and grateful regards to my advisor, Professor Heungjoo Shin. He always guided me to improve not only the quality of my research but the attitude as a member of society during the master's course. In a word, it is not too much to say that I could not have accomplished this goal without his concerns and caring. I also feel enormous gratitude to the committee members, Professor Jaesung Jang and Professor Hooneui Jeong for giving suggestions and assistances during the thesis presentation. Thanks to their help, I could successfully complete this thesis.

And I want to give thanks to all MNIS Lab members, Deepti Sharma, Yeongjin Lim, Jongmin Lee, Beomsang Kim, Seungwook Lee, Sanghee Jeong and Taejung Kim. I really appreciate them for help and consideration during my master's course in UNIST. Owing to their inspiring attitudes and happy time we spent together, I had a great experience. Although they already graduated and left, I also want to appreciate my graduated seniors, Jisoo Hong and Junyoung Seo. When I got stressed out, they helped and advised me with warm words. It was a stroke of luck that I met MNIS Lab members.

Moreover, I owed special thanks to my best friends. I really feel grateful for their continuous supports and strong trusts to Euidae Jeong, Gyoungseo Doo, Jaehong Gwon, Sanggi Do, Seungjae Baek, Seungjae Yang and Younghyun Lim. And I am thankful for my old friends as well. Even if it has been somewhat difficult to meet them, I always appreciate for cheering and advice to Chanhyuk Ahn, Inwoo Lee, Namhyuk Kim, Seonjoong Kim and Wongi Jeong. When I got depressed in UNIST, the best solution to recover from stress was to contact or hang out with them. They are the most valuable gifts in my life.

Above all, of course, I always owe a real debt of gratitude for my family. Whenever I felt lacked the courage during the master course, they have believed and supported me with endless love. At all times, they are my only reason for living. Though I feel sorry about the present that I cannot tell my achievement to my late father, I always feel gratitude, reverence and love to him. Owing to the dedication and love of my family, I could finish my master's course.

Finally, I return my grateful acknowledgement to all these precious people of mine.